ZAMM · Z. Angew. Math. Mech. **92**, No. 9, 683 – 708 (2012) / **DOI** 10.1002/zamm.201200097

Retrospective

Prandtl-Tomlinson model: History and applications in friction, plasticity, and nanotechnologies

V. L. Popov* **and J. A. T. Gray**

Berlin University of Technology, 10623 Berlin, Germany

Received 4 April 2012, accepted 31 May 2012
Published online 5 July 2012

Communicated by Holm Altenbach

Key words Prandtl-Tomlinson model, retrospective.

One of the most popular models widely used in nanotribology as the basis for many investigations of frictional mechanisms on the atomic scale is the so-called Tomlinson model consisting of a point mass driven over a periodic potential. The name "Tomlinson model" is, however, historically incorrect: The paper by Tomlinson from the year 1929 which is often cited in this context did not, in fact, contain the model known as the "Tomlinson model" and suggests, instead, an adhesive contribution to friction. In reality, it was Ludwig Prandtl who suggested this model in 1928 to describe the plastic deformation in crystals and dry friction. Staying in line with some other researchers, we call this model the "Prandtl-Tomlinson model," although the model could simply and rightly be dubbed the "Prandtl model." The original paper by Ludwig Prandtl was written in German and was not accessible for a long time for the largest part of the international tribological community. The present paper is a historical introduction to the English translation of the classical paper by Ludwig Prandtl. It gives a short review of the model as well as its properties, applications, and extensions from the contemporary viewpoint.

1 Introduction

In 1928, Ludwig Prandtl suggested a simple model for describing plastic deformation in crystals [1]. He considered the process of plastic deformation and abstracted it stepwise to a model in which a stage with many elastically coupled "atoms" is moved along a periodic potential. To start with, Prandtl simplifies it even further and considers only the one-dimensional movement of a point mass being dragged in a periodic potential by means of a spring with a constant velocity v_0 and damped proportional to velocity (Fig. 1a)[1]:

$$m\ddot{x} = k\left(v_0 t - x\right) - \eta\dot{x} - N\sin\left(2\pi x/a\right). \tag{1}$$

Here, x is the coordinate of the body, m its mass, k the stiffness of the pulling spring, η the damping coefficient, N the amplitude of the periodic force, and a the spatial period of the potential. In the case of a very soft spring, the motion over one or several periods does not change the spring force F, which can be considered to be constant. In this case, the model can be simplified to the form

$$m\ddot{x} = F - \eta\dot{x} - N_0\sin(2\pi x/a). \tag{2}$$

This is illustrated in Fig. 2. After analyzing the one-dimensional model (1), Prandtl generalizes it back to a system with many independent "atoms" coupled to a stage as well as to an ensemble of "atoms" with different coupling stiffnesses, and then even to an ensemble of "systems," which from a macroscopic point of view simulates a multi-contact situation.

Over many years, the basic models (1) or (2) have been referred to as the "Tomlinson model" and the paper [2] by Tomlinson from 1929 has been cited in this connection. However, the paper by Tomlinson did not contain the above model. In the following, due to the long historical tradition, we will call this model the "Prandtl-Tomlinson model".

The model from Prandtl describes many fundamental properties of dry friction. Actually, we must apply a minimum force to the body so that a macroscopic movement can even begin. This minimum force is none other than the macroscopic

* Corresponding author E-mail: v.popov@tu-berlin.de

[1] Prandtl visualized this system with a mechanical model consisting of a wave-like surface upon which a heavy roller rolls back and forth. The elastic force is realized by the springs whose ends are fastened to a gliding stage.

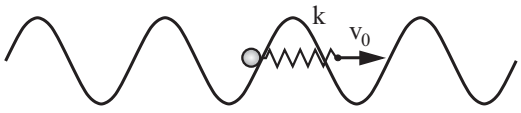

Fig. 1 The Prandtl model: A point mass dragged in a periodic potential.

Fig. 2 Simplified Prandtl model in the case of a very soft spring (modeled here by a constant force).

force of static friction. If the body is in motion and the force reduced, then the body will generally continue to move, even with a smaller force than the force of static friction, because it already possesses a part of the necessary energy due to its inertia. Macroscopically, this means that the kinetic friction can be smaller than the static friction, which is a frequently recurring characteristic of dry friction. The force of static friction in the model described by Eq. (1) is equal to N.

The success of the model, variations and generalizations of which are investigated in innumerable publications and are drawn on to interpret many tribological processes, is due to the fact that it is a simplistic model that accounts for two of the most important fundamental properties of an arbitrary frictional system. It describes a body being acted upon by a periodic conservative force with an average value of zero in combination with a dissipating force which is proportional to velocity. Without the conservative force, no static friction can exist. Without damping, no macroscopic sliding frictional force can exist. These two essential properties are present in the PT-model. In this sense, the PT-model is the simplest usable model of a tribological system. It is interesting to note that the PT-model is a restatement and further simplification of the view of Coulomb about the "interlocking" of surfaces as the origin of friction.

The PT-model was designed for understanding plasticity [1], but its extensions and variations are widely used for understanding processes of various physical natures, including dislocations in crystals (Frenkel-Kontorova model [3, 4]), atomic force microscopy [5], solid-state friction [6], control of friction by chemical and mechanical means as well as in the design of nano-drives [7, 8], and handling of single molecules [9].

In his original paper, Ludwig Prandtl considered not only the simplest deterministic form of the model, but also the influence of thermal fluctuations. He was the first "tribologist" who came to the conclusion that thermal fluctuations should lead to a logarithmic dependency of the frictional force on velocity.

The rest of this paper is organized as follows: In Sect. 2 we describe the main findings of the paper by Prandtl, in Sect. 3 we discuss further well-known extensions and applications of the Prandtl model. We would like to stress that this paper is not based on a deep historical recherché and all following discussions make no claims of being complete.

2 Results of Prandtl

Prandtl notes, first, that the movement of the mass point does not follow the movement of the stage continuously, provided that the pulling spring is soft enough. For small pulling velocities, this condition of *elastic instability* reads

$$k < N\frac{2\pi}{a}. \tag{3}$$

In this case, a hysteresis is observed when the stage is moved over large distances back and forth. This is, according to Prandtl, the physical reason for plastic hysteresis. Since the 1980s it has been known in the nanotribological community that the existence of elastic instabilities is indeed the necessary condition for a finite static frictional force in atomic scale friction [5, 24]. If the stiffness k is larger than the critical value, the average spring force (interpreted as a macroscopic force of friction) becomes identically zero. This property has been proven exactly for an arbitrary periodic potential [11]. A direct consequence of this property is that if a large number of "atoms" is connected with a rigid movable stage (Fig. 3), then the tangential force vanishes at any time moment, provided the stiffness is overcritical and the periods of structures are incommensurate. In the literature on nanotribology, this effect is known as "superlubricity" [27]. Superlubricity can be

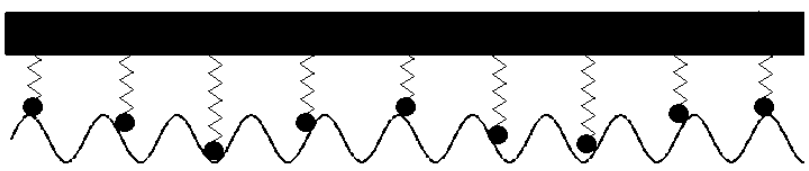

Fig. 3

observed either if the crystal lattices of two contacting bodies are incommensurate or if the lattices are rotated with respect to one another [25]. Note that the similarity of the term superlubricity to the terms superconductivity and superfluidity is misleading, because it refers only to the *static* friction force. The interaction with electrons and phonons will generally lead to a final, velocity dependent frictional force. However, in dielectric materials at very low temperatures, an effect similar to true superfluidity may take place, which in [29] was called *superslipperiness*.

If the loading is non-monotonous, then the exact state of the system at any moment of time depends on its prehistory. In the case of an ensemble of particular systems with different parameters, this state can be very complicated. Prandtl poses the question of whether it is possible to restore the *virgin state* in which all the "atoms" are again in their initial non-stressed positions. With very simple arguments he shows that if the stage starts to oscillate with large amplitude and the amplitude then decreases *slowly*, then each "atom" in the ensemble finally comes to the neutral, non-stressed position and the system returns to the virgin state. He compares this result with demagnetization through slowly decreasing oscillating magnetic fields, first studied by E. Madelung [12].

Prandtl further considers the properties of the model at finite temperatures. The principle idea exploited by Prandtl is to calculate back and forth mass currents due to thermal fluctuations. If the height of the periodic potential in (1) is U_0 and the spatial period a, then in a first approximation, a spring force F will change the heights of the "left" and "right" potential barriers and they will become $U_1 = U_0 + Fa/2$, $U_2 = U_0 - Fa/2$, thus, leading to a total sliding velocity $\dot{v}$ of

$$\dot{v} = C\left(\mathrm{e}^{-(U_0 - Fa/2)/k_B T} - \mathrm{e}^{-(U_0 + Fa/2)/k_B T}\right), \tag{4}$$

where k_B is the Boltzmann constant and T the absolute temperature. For *medium* forces satisfying the condition

$$kT \ll Fa/2 \ll U_0, \tag{5}$$

the back transitions in (4) can be neglected and we have $\dot{v} = C\mathrm{e}^{-(U_0 - Fa/2)/k_B T}$. Solving this equation for F

$$F = 2U_0/a + (2k_B T/a)\ln(\dot{v}/C) \tag{6}$$

gives the famous logarithmic dependency of the frictional force on velocity [6], which is found both at the atomic scale [5] and at the macro scale [17]. Note that the coefficient of the logarithmic term is proportional to the absolute temperature. For extremely small forces

$$Fa/2 \ll kT, \tag{7}$$

the velocity is a linear function of the force

$$v = C\mathrm{e}^{-U_0/k_B T}\left(\mathrm{e}^{Fa/2k_B T} - \mathrm{e}^{-Fa/2k_B T}\right) \approx C\mathrm{e}^{-U_0/k_B T}\frac{Fa}{k_B T}, \tag{8}$$

as it should be from general thermodynamic principles. The exact solution of (4) with respect to F has the form

$$F = a(T)\cdot \operatorname{asinh}(v/v_c), \tag{9}$$

which has been confirmed recently by direct molecular dynamic simulations [16]. Particularly for very small velocities, Prandtl comes to the "noteworthy result" that the force is proportional to the deformation rate. Thus, "a resistance of the same type as the drag in a fluid exists." In this viscous region he comes to the conclusion that the viscosity is an exponential function of temperature and pressure (as shown in experiments by Bridgeman [30]).

For larger forces in the region $Fa/2 \approx U_0$, a more detailed analysis is needed. In this case, the back transitions can be neglected. If the initial potential is approximated as

$$U = U_0\left[\frac{3}{2}\left(\frac{2x}{a}\right) - 2\left(\frac{2x}{a}\right)^3\right] \tag{10}$$

(preserving the distance $a/2$ between the minimum and the adjacent maximum and the height U_0 of the potential barrier), then in the presence of a constant force, the potential energy will be

$$U = U_0\left[\frac{3}{2}\left(\frac{2x}{a}\right) - 2\left(\frac{2x}{a}\right)^3\right] - Fx. \tag{11}$$

The distance between the minimum and the maximum is equal to

$$\tilde{a} = \frac{a}{2}\left(1 - \frac{1}{3}\frac{Fa}{U_0}\right)^{1/2} \tag{12}$$

and the energy difference is

$$\Delta U = U_0\left(1 - \frac{1}{3}\frac{Fa}{U_0}\right)^{3/2}. \tag{13}$$

Therefore, for the macroscopic sliding velocity, we obtain

$$v \approx C\mathrm{e}^{-\Delta U/T} = C\exp\left(-U_0\left(1 - \frac{1}{3}\frac{Fa}{U_0}\right)^{3/2} \Big/ k_B T\right). \tag{14}$$

Solving for F under the condition $\ln(v/C) < 0$ gives

$$F = \frac{3U_0}{a}\left[1 - \left(\frac{k_B T}{U_0}\right)^{2/3}\left|\ln\frac{v}{C}\right|^{2/3}\right]. \tag{15}$$

Thus, the Prandtl model predicts the following temperature dependence of the force of friction

$$F = C_1 - C_2 T^{2/3}. \tag{16}$$

This dependency, first found by Prandtl, has been rediscovered in the context of atomic force microscopy [13] and has been observed experimentally [18, 26]. It is interesting to note that the determination of the thermally activated sliding velocity formally coincides with many problems in chemical kinetics. The results of Prandtl, therefore, also find a place in these areas of application [9].

All of the above mentioned results of the paper have been obtained by Prandtl in a much more rigorous way as briefly summarized above. As already mentioned, Ludwig Prandtl considered an ensemble of systems and solved a kinetic equation for them in a very similar way to how it is done by the contemporary researchers [13]. The Eq. (1) in his paper, which in contemporary notations would read

$$\frac{dP(x,t)}{dt} = \frac{1}{\tau}\left((1 - P(x,t))\,\mathrm{e}^{-\frac{U_2(x)}{k_B T}} - P(x,t)\,\mathrm{e}^{-\frac{U_1(x)}{k_B T}}\right), \tag{17}$$

(with $P(x,t)$ being the probability for the atoms to take the position x in the potential relief), is nothing other than the kinetic equation for the ensemble of systems and the following treatment is essentially equivalent to solving the Fokker-Planck equation. The derivations around Eq. (20) of Prandtl's paper give, in the end, essentially the same results as were found by Kramers in his classical paper on kinetics of chemical reactions [19]. However, one must admit that the calculations by Prandtl and his terminology are very difficult to follow. This may be one of the reasons why his paper has not had the impact to the development of science that it deserves. Now, it is of course possible to directly solve Eq. (1) with additional stochastic forces modeling thermal fluctuations. A very good review of such "molecular dynamic" investigations of the PT-model can be found in an excellent recent paper by Martin Müser [16]. Prandtl was concentrated on the study of quasi-static movements and creep, so he did not investigate the dynamic properties of the model. An overview of basic dynamic properties is given in [11].

It is interesting to note that the entire paper by Prandtl is devoted to the discussion of plasticity. Only at the end of his paper, does he come to a discussion of friction and notes that "... our conceptual model is also suitable for the treatment of kinetic friction between solid bodies." In this connection, he cites experimental results on the logarithmic dependence of the frictional force on the sliding velocity and states that "the law that frictional force increases with the logarithm of velocity is confirmed very well in a large range of velocities." He finally speculates on the reasons for the approximate proportionality of the frictional force to the normal force and suggests two physical reasons for this: On the one hand, the effective contact area of both bodies increases with the normal force; and on the other hand, through the increase in surface pressure, the molecules of both bodies are brought into closer proximity, thus, a force field with a larger wave amplitude is present. These dependencies of the local potential amplitude on the normal force have in the meantime been investigated

experimentally [24] and theoretically and are indeed considered to be one of the reasons for the validity of Coulomb's law of friction [28].

3 Applications and extensions of the Prandtl-Tomlinson model

1. The initial application of the model was the understanding of plastic deformation and deformation creep at finite temperatures.

2. Historically, the main application of the Prandtl model has been found in nanotribology, especially for the understanding of experiments with atomic force microscopes (for review see [5]).

3. The equation of type (2) – rewritten in another notation –

$$\left(\frac{\hbar C}{2e}\right)\ddot{\varphi} = j - \left(\frac{\hbar}{2eR}\right)\dot{\varphi} - j_0 \sin\varphi, \tag{18}$$

describes the dynamics of a single Josephsohn contact [20]. In Eq. (18), $\hbar$ is Planck's constant, φ is the phase difference between contacting superconductors, C and R are the respective contact capacity and ohmic resistance, e is the elementary charge, and j_0 is the maximum contact current. The mathematical equivalence of the two problems means that the effects seen in Josephsohn's contacts must be observed in tribological systems whose microscopic model is described by Eq. (2). One of the effects is in the modification of the current-voltage characteristic of a Josephsohn's contact undergoing an external periodic perturbation. The modification is in the appearance of plateaus where the voltage is rigorously constant (modern quantum voltage standard is based on this effect). An analogy to this effect in terms of tribology is the appearance of a plateau of a constant average velocity of a body in the presence of a periodic oscillating force. These plateaus play a key role in the further discussion of nanomachines.

4. One further extension of the simple PT-model is to consider a number of "atoms" which are elastically coupled with both the moving stage and with each other (Fig. 4). This model has been proposed by Frenkel and Kontorova [3, 4] to describe dislocation-based plastic deformation in crystals.

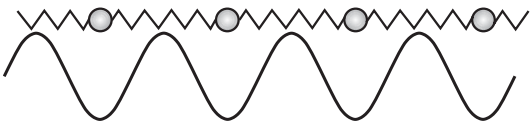

Fig. 4 Kontorova-Frenkel model.

Considering the series of elastically coupled atoms as an elastic continuum, one gets the following equation of motion of the system

$$\frac{\partial^2 u}{\partial t^2} = c^2 \frac{\partial^2 u}{\partial x^2} - \alpha \frac{\partial u}{\partial t} - R \sin\left(\frac{2\pi u}{a}\right) + f, \tag{19}$$

where u is the tangential displacement of a mass point with the initial coordinate x. α is a damping constant, f is the force density acting homogeneously on all mass points (not shown in Fig. 3), c is the sound velocity in the elastically coupled chain (without interactions with the periodic potential and the stage) and R is a constant characterizing the amplitude of the periodic potential. Equation (19) is also known as the Sine-Gordon equation. Its static solutions correspond to dislocations in a crystal. Moving solutions of the form $u = u(x - vt)$ lead to the equation

$$\left(c^2 - v^2\right)\frac{\partial^2 u}{\partial x^2} + \alpha v \frac{\partial u}{\partial x} = R \sin\frac{2\pi u}{a} - f, \tag{20}$$

which is an equation precisely of the same form as the simplified PT-equation (2) (only the time should be replaced by x and the coordinate by u).

5. We consider an automobile that is powered by a single-cylinder internal combustion engine and drives downhill at an angle of α to the horizontal plane. Due to the fact that the fuel injection and combustion is coupled to a distinct phase angle of the piston and, therefore, to the angle of the crank shaft, one can consider the moment that the motor exerts on the axle before the gearbox as a function of the angle θ: $M^* = M^*(\theta)$. We can write this function as

$$M^*(\theta) = M_1 + M_2 \sin\theta. \tag{21}$$

If a gearbox with a gear ratio of n is connected between the motor and the wheel axle, then the moment exerted on the axle is equal to $M = nM^*(\varphi/n)$. Neglecting the moment of inertia of the wheels, one obtains the following equation of motion for the automobile

$$\ddot{\phi} + \frac{\gamma}{m}\dot{\phi} = \left(\frac{g}{r}\sin\alpha + \frac{nM_1}{mr^2}\right) + \frac{nM_2}{mr^2}\sin\left(\phi/n\right), \tag{22}$$

where φ is the angle of rotation of the wheel, r the radius of the wheels, m the mass of the automobile, and g the gravitational acceleration. Thus, the simplest case of engine braking is also described by the PT-model!

6. Most of the ways of generating directed motion of molecular objects discussed in literature are based on the interaction between a driven object and an inhomogeneous, commonly periodically structured substrate. The latter can be either asymmetric or symmetric. In the former case, the directed motion can be only unidirectional; it is fixed by the interaction between the substrate and the object following the "ratchet-and-pawl" principle (see [15]). In the latter case, the direction of motion is originally not fixed and is determined dynamically. An example of this kind of a dynamically driven engine was given in [7] and [8]. The models utilized in these works are nothing but a generalized PT-model with oscillating forces.

7. Very thin layers of liquid between crystalline solids have a tendency to undergo layering transitions [21]. Under these boundary lubrication conditions, the fluid takes on the properties of the solid state. The sliding in this case can also be described by a generalized PT-model [22].

8. Further generalizations are very numerous and include, for example, the substitution of a periodic potential by a stochastic one, thus, producing a random PT-model [22]. This allows the transformation of the viscous friction at the nano-scale to a Coulomb-like friction at the macro-scale to be considered by means of a sort of renormalization technique.

4 Conclusion

Ludwig Prandtl is known foremost for his contributions to hydrodynamics. However, like many other accomplished scientists, he provided important contributions to scientific areas which were not the main field of his activities. One of these contributions is the paper on the theory of plasticity, analyzed with what we now call the Prandtl-Tomlinson model. Prandtl investigated problems which still remain a subject of scientific investigation until today. The model has played a very prominent role in the history of science, especially tribology, which can be compared with other classical models, such as the contact theory by H. Hertz or the lubrication theory by Petrov and Reynolds. With the publication of an English translation of the classical paper by Prandtl, we would like to honor this outstanding contribution from an outstanding scientist.

References

[1] L. Prandtl, Ein Gedankenmodell zur kinetischen Theorie der festen Körper, Z. Angew. Math. Mech. **8**, 85–106 (1928).
[2] G. A. Tomlinson, A molecular theory of friction, Philos. Mag. **7**, 905–939 (1929).
[3] T. A. Kontorova and Y. I. Frenkel, On the theory of plastic deformation and crystal twinning (in Russian), Zh. Eksp. Teor. Fiz. **8**(1), 89–95 (1938).
[4] T. A. Kontorova and Y. I. Frenkel, Zh. Eksp. Teor. Fiz. **8**(12), 1340–1348 (1938).
[5] E. Meyer, R. M. Overney, K. Dransfeld, and T. Gyalog, Nanoscience: Friction and Rheology on the Nanometer Scale (World Scientific, Singapore, 1998).
[6] M. H. Müser, M. Urbakh, and M. O. Robbins, Statistical mechanics of static and low-velocity kinetic friction, edited by I. Prigogine and S. A. Rice, Adv. Chem. Phys. **126**, 187–272 (2003).
[7] M. Porto, M. Urbakh, and J. Klafter, Atomic scale engines: cars and wheels, Phys. Rev. Lett. **84**, 6058—6061 (2000).
[8] V. L. Popov, Nanomachines: Methods of induce a directed motion at nanoscale, Phys. Rev. E **68**, 026608 (2003).
[9] O. K. Dudko, G. Hummer, and A. Szabo, Intrinsic rates and activation free energies from single-molecule pulling experiments, Phys. Rev. Lett. **96**, 108101 (2006).
[10] A. Barone, F. Esposito, C. J. Magee, and A. C. Scott, Theory and applications of the sine-gordon equation, Riv. Nuovo Cimento **1**(2), 227–267 (1971).
[11] V. L. Popov, Contact Mechanics and Friction. Physical Principles and Applications (Springer, Berlin, Heidelberg, New York, 2011).
[12] E. Madelung, Über Magnetisierung durch schnell verlaufende Ströme, Göttingen 1905, Ann. Phys. (Berlin), **17**, 861 (1905).

[13] O. K. Dudko, A. Filippov, J. Klafter, and M. Urbakh, Dynamic force spectroscopy: a Fokker–Planck approach, Chem. Phys. Lett. **352**, 499–504 (2002).
[14] A. E. Filippov and V. L. Popov, Fractal Tomlinson model for mesoscopic friction: From microscopic velocity-dependent damping to macroscopic Coulomb friction, Phys. Rev. E **75**, 027103 (2007).
[15] P. Reimann, Brownian motors: noisy transport far from equilibrium, Phys. Rep. **361**, 57–265 (2002).
[16] M. H. Müser, Velocity dependence of kinetic friction in the Prandtl-Tomlinson model, Phys. Rev. B **84**, 125419 (2011).
[17] J. H. Dieterich, Modeling of rock friction. 1. Experimental results and constitutive equations, J. Geophys. Res. **84**(B5), 2161 (1979).
[18] Y. Sang, M. Dubé, and M. Grant, Phys. Rev. Lett. **87**, 174301 (2001).
[19] H. A. Kramers, Brownian motion in a field of force and the diffusion model of chemical reactions, Physica (Utrecht) **7**, 284–304 (1940).
[20] A. Barone and G. Paterno, Physics and Applications of the Josephson Effect (Wiley & Sons, Hoboken, 1982).
[21] P. A. Thompson, G. S. Grest, and M. O. Robbins, Phase transitions and universal in confined films, Phys. Rev. Lett. **68**, 3448–3451 (1992).
[22] V. L. Popov, A theory of the transition from static to kinetic friction in boundary lubrication layers, Solid State Commun. **115**, 369–373 (2000).
[23] E. Gnecco, R. Bennewitz, T. Gyalog, C. Loppacher, M. Bammerlin, E. Meyer, and H. J. Guntherodt, Velocity dependence of atomic friction, Phys. Rev. Lett. **84**, 1172–1175 (2000).
[24] E. Gnecco, R. Bennewitz, and E. Meyer, Transition from stick-slip to continuous sliding in atomic friction: Entering a new regime of ultralow friction, Phys. Rev. Lett. **92**, 134301 (2004).
[25] M. Dienwiebel et al., Superlubricity of graphite, Phys. Rev. Lett. **92**, 126101 (2004).
[26] L. Jansen, H. Hölscher, H. Fuchs, and A. Schirmeisen, Temperature dependence of atomic-scale stick-slip friction, Phys. Rev. Lett. **104**, 256101 (2010).
[27] H. Hölscher, A. Schirmeisen, and U. D. Schwarz, Principles of atomic friction: from sticking atoms to superlubric sliding, Philos. Trans. R. Soc. Lond. A **366**, 1383–1404 (2008).
[28] S. F. Cheng, B. Q. Luan, and M. O. Robbins, Contact and friction of nanoasperities: Effects of adsorbed monolayers, Phys. Rev. E **81**, 016102 (2010).
[29] V. L. Popov, Superslipperiness at low temperatures: Quantum mechanical aspects of solid state friction, Phys. Rev. Lett. **83**, 1632–1635 (1999).
[30] P. W. Bridgeman, Proc. Am. Acad. Arts Sci. **61**, 57 (1926).

ZEITSCHRIFT FÜR ANGEWANDTE MATHEMATIK UND MECHANIK
INGENIEURWISSENSCHAFTLICHE FORSCHUNGSARBEITEN
Band 8 April 1928 Heft 2

Inhalt:

MAIN ARTICLES

A Conceptual Model to the Kinetic Theory of Solid Bodies.

by **L. PRANDTL** in Göttingen.

(Translated from German original by Valentin L. Popov and Joshua Gray, Berlin University of Technology)

1. Preliminary remarks regarding the experimental facts. If one investigates the relationship between the stresses and deformations in a tensile/compression test more closely, one can differentiate between several irreversible contributions alongside a reversible contribution to deformation. The reversible contribution is none other than that which is commonly known as the purely elastic contribution. Of the irreversible contributions, one is dependent on the loading history but not on the respective time, while the other exhibits a distinct time dependence. The former is called elastic hysteresis, analogous to a similar occurrence in the magnetization of iron and steel. The latter, the time-dependence, encompasses the aspects of aftereffects, the dependence of yield stress on deformation speed, and some slow changes in state, which consist of changes in the yield point[2].

For magnetic hysteresis, E. Madelung established several noteworthy laws in his dissertation[3]. As these have also been proven for elastic hysteresis, they shall be mentioned here. I will present these laws immediately in a form compatible for elastic hysteresis, and thereby, explicitly mention that in the following, time contributions will not be accounted for; these contributions are usually insignificant at moderate loading and if the experiment is not carried out too slowly. First, a definition:

For every change in the direction of stress, there exists a change in direction of deformation. This means that if the stress initially increases and then once again decreases, then the same is true of the deformation. The curve presented in the $\sigma - \varepsilon$ plane ($\sigma =$ stress; $\varepsilon =$ strain) contains a kink for every change in direction, provided that the curve does not turn back upon itself. Every such point is called a "reverse point."

Now, the expressions:

1. Every $\sigma - \varepsilon$ curve which emanates from a reverse point A (α in Fig. 1) is clearly defined by the coordinates of this reverse point.
2. If a point on the curve α becomes a new reverse point B by changing the direction of the loading curve, then the reverse loading curve β originating at B ends up once again at the first reverse point A.
3. If the curve β, originating at the reverse point B, continues through the first reverse point A, then it continues as would the curve which originally reached point A; the curve continues as if the cycle ABA had never taken place.

[2] Because any experiments require a certain time to be carried out, the time-dependent effects are not able to be completely separated by those independent of time. The distinction is, therefore, more practical in nature.

[3] Ueber Magnetisierung durch schnell verlaufende Ströme. Göttingen 1905. Ann. d. Phys. 17 (1905), S. 861.

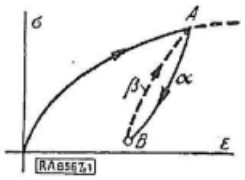

Fig. 1

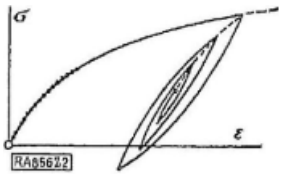

Fig. 2

According to the third statement, it follows that, among other things, if one allows the stress to proceed as a form of damped oscillation, where the $\sigma - \varepsilon$ curve produces a type of spiral (Fig. 2), a new $\sigma - \varepsilon$ curve originating at the center of the spiral crosses all of the reversible points on one side of the spiral. This "intersecting curve" consists of many pieces of the individual "loading curves" and, therefore, adheres to a different law than those mentioned.

Previously, I had these laws verified by Dr. S. Berliner[4] on cast-iron rods which showed strong hysteresis. He was able to confirm them very well in all cases in which no time-dependent contributions were present. In particular, it can be shown that the intersecting curves fall practically completely over the initial loading curve, the so-called virgin curve. Also, with respect to the absence of time-dependent processes, the state of the middle point of a spiral corresponds to the initial unloaded state.

With respect to the time-dependent processes, I would like to remain brief here and restrict myself only to the dependence of the yield stress on the deformation speed. Later, I will come back to the elastic aftereffects as well as slow changes in state, to which crystal regeneration and recrystallization belong. The changes in stress due to changes in deformation speed, when the slow side effects caused by changes in state are neglected, can be set proportional to the logarithm of the deformation speed. So, this means that a geometric series of deformation speeds belongs to an arithmetic series of stress increases. Increases in stress are, thereby, calculated from a $\sigma - \varepsilon$ curve having a constant deformation speed. This law, for instance, is found to be correct within a large range of mild steel[5], however, is also mostly correct in other cases.

2. The model. After the introductory comments, I will transition to the subject at hand. It deals with the following questions: Can these processes be understood from a kinetic standpoint? Is there a useable theory for accomplishing this? I once laid these questions before me, excited by the aforementioned experimental work, and found a satisfactory way in which one can, through pertinent simplifications, come upon these things also by calculations. Th. v. Kármán reported these in his article "Physikalische Grundlagen der Festigkeitslehre" in the Enzyklopädie der mathematischen Wissenschaften[6] 1913. At that time, I myself produced no publications of my own on the subject due the demands on me regarding aerodynamics. In the meantime, the physical research into solid bodies, through studies of crystalline structures as well as that of atomic physics, has once again become up-to-date (to pure physicists it has only now, for the first time, really become up-to-date). Thus, it looked as if the time had come to retrieve my old work. In doing this, I also succeeded in several improvements regarding the mathematics[7].

Now, we must depart from the very complicated processes of the inelastic deformations of a molecular lattice and use a sufficiently simplified method which does not sacrifice the important aspects of the problem. We use our physical knowledge and say that one observes neither hysteresis nor aftereffects in an undisturbed crystal. Therefore, the aspects most responsible for hysteresis and aftereffects in polycrystals are the grain boundaries between the individual crystals, followed by irregularities in the internal lattice structure. Following a permanent deformation, such structural disturbances to the lattice are present in multitudes, even in the internal of the crystal. For grain boundaries, as well as structural disturbances, the following is valid: two lattices have a more or less irregular boundary; between them, there are several molecules under the influence of the attraction and repulsive forces of both lattices without belonging to either lattice structure. Every one of these molecules could be bound to one lattice stronger than the other; it affects the generality of the observation very little if we assume that all of these loosely bound molecules are elastically attached to one of the two lattices. Now, during a deformation, the force field of the other lattice would pass over the attached molecules and, thereby, bring them into alternating equilibrium states. For simplification, we make one further restriction saying that every molecule can exhibit only one degree of freedom. In reality, however, this does not apply. The particles will exhibit movement in mostly one direction, the one in which they are most easily displaced, so that our restriction would, in general, not do much harm.

[4] Ueber das Verhalten des Gußeisens bei langsamen Belastungswechseln. Diss. Göttingen 1906. Ann. D. Phys. 20 (1906), S. 527.

[5] H. Cassebaum, Ueber das Verhalten von weichem Flußstahl jenseits der Proportionalitätsgrenze. Diss. Göttingen 1911. Ann. d. Phys. IV, 34 (1911), S. 106.

[6] Encyl. Bd. IV, Artikel 31, S. 767 u. f.

[7] A considerable amount of this arose out of Winter Semester 1921/22, as I conducted a seminar on this subject for my students.

With this, we arrive at our conceptual model: We imagine two parallel straight edges sliding against one another, of which one (A) contains many elastically mounted point masses at regular or irregular intervals which can oscillate parallel to the axis of the straight edge, while the second straight edge (B) exerts a force field, as if it were to correspond to a somehow crookedly cut lattice. In a force field, which we can think of as being generated by the centers of attraction and repulsion at the positions of the atoms in the lattice (as is really the case in an ion lattice), we consider only the force components in the direction of the point masses. This means that we consider alternating forces to the right and to the left with a regular or irregular wavelike intensity curve. Thereby, the period of the force field should be incommensurate with the period of the resting positions of the point masses. The deformation of the solid body will be presented as the displacement of straight edge A with respect to straight edge B; the force or stress necessary for the deformation of the solid body is presented by the total force, which is the summation of the forces acting on the individual point masses.

In order to get an idea of what happens with this model, we want to first consider a singular point mass. Its equilibrium positions are the points where the elastic force P_A, which acts on the point mass from straight edge A, is equal and opposite to that which acts on the point mass from the field of force B, that being P_B.

The graphical representations in Fig. 3 and Fig. 4 give a good overview of the possibilities at hand. The forces P_A and P_B are plotted as straight lines and wave lines as a function of x parallel to the straight edge (a non-linear relationship for the elastic force would be fundamentally possible, but would change nothing significantly). A point mass with a resting position at C finds its equilibrium position under the influence of the field of force at position D, where equilibrium exists between P_B and $-P_A$. Were A to now be displaced with respect to B by a magnitude of ξ (out of graphical reasons, we leave the waveforms where they are and move the lines), the new equilibrium state is reached at D', obtained by displacing C by ξ to the point C'. If the relationships are as shown in Fig. 3, there exists for every displacement ξ a unique equilibrium state of the point mass. In the case of Fig. 4, however, where the force field is stronger and the elastic bond weaker, cases present themselves in which several equilibrium states are possible. In the case shown, there are three; D' and D''' are stable equilibrium states, as one can easily recognize by considering the forces occurring for a small displacement of the point mass. The equilibrium state D'', lying in-between, is instable.

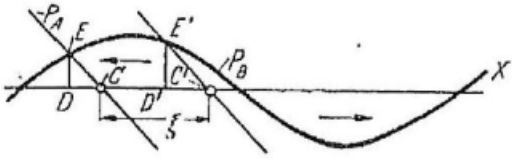

Fig. 3

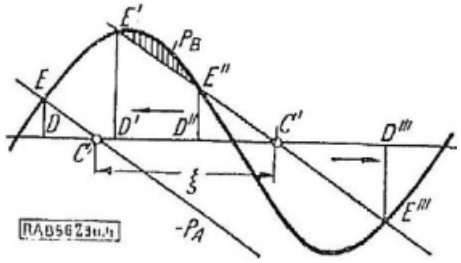

Fig. 4

If one lets the displacement ξ now increase from zero, then the equilibrium state D' remains as it is until the line P_A intersects the waveform P_B. Here, the instable state D'' coincides with that of state D', causing the point mass to swing over to D''' and remain there after its oscillatory energy has been damped. Now, if ξ were to once again decrease, the point mass does not immediately swing back to its old position, but rather it remains near its new position until the line P_A reaches the lowest point of intersection with the curve. Only then, can the old position once again be reached by means of a new transition. So, the essential point is that different equilibrium states and different forces result for movement in each direction. As the forces are the most important aspect to us for the application of the model, we want to move on to another representation where the forces act as a function of the displacement ξ. For this, we need only plot every segment DE from the associated C perpendicular to the x-axis as CF. Figure 5 and Fig. 6 arise from Fig. 3 and Fig. 4; in these new figures, the three related equilibrium states now lie on a line perpendicular to the axis (F', F'', and F'''). In the case shown in Fig. 5, the same force trend results from movement in both directions. In the case shown in Fig. 6, on the other hand, the trend for the initial movement is shown in Fig. 7 and that of the return movement in Fig. 8.

The experimental model in Fig. 9 allows the individual processes to be clearly seen. The force field is replaced by a wavelike surface upon which a heavy roller rolls back and forth (the slope of the trajectory of the center of mass represents the force P_B). The elastic force is realized by the springs F_1 and F_2, whose ends are fastened to the straight edge A. If straight edge A is dragged against straight edge B, then as long as the springs are not too strong, the equilibrium position of the roller at the summit of the wavelike surface is instable and the processes shown in Fig. 6 to Fig. 8 occur. Thereby, one can let the sketch in Fig. 6 (as well as those in Fig. 7 and Fig. 8) be produced by the model itself using the following adjustments. On the right side of the model, there is a perpendicular attachment in which a sliding piece G moves carrying

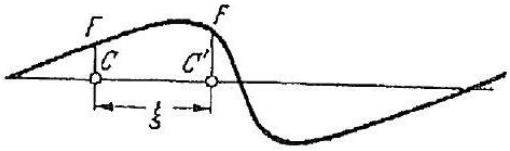

Fig. 5

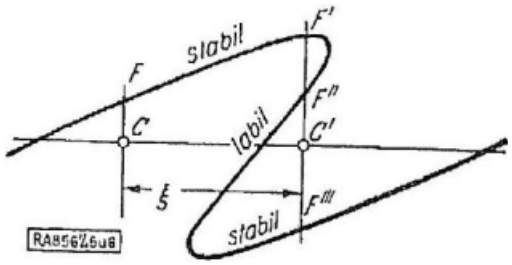

Fig. 6

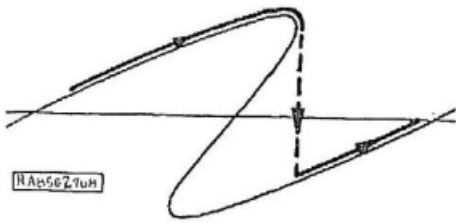

Fig. 7

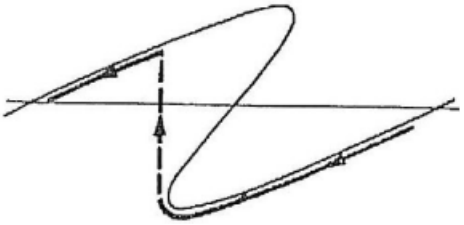

Fig. 8

a pointer Z. The sliding piece is carried by a cord which is run over rollers and whose opposite end is attached to a weight M. In doing this, the perpendicular path of the sliding piece and the pointer is equal, with small deviations, to the change of length of the springs, or about proportional to the spring force. The horizontal movement of the pointer, however, corresponds to the displacement of straight edge A, so that the values in Fig. 6 are essentially reproduced. As the straight edge is slowly moved to the right, the pointer draws the line in Fig. 7 onto the chart; as the straight edge moves to the left, the pointer draws the line in Fig. 8. The jump from one section of the curve to the next takes place, of course, under heavy oscillations. The instable equilibrium positions can also be obtained; due to the inevitable friction it is possible, with a little caution, to place the mass M in every instable position (the pointer sits in the middle section of the curve). It may be mentioned that one can, of course, also obtain the curve in Fig. 5 with the application of stiffer springs, although this type is not of interest to us.

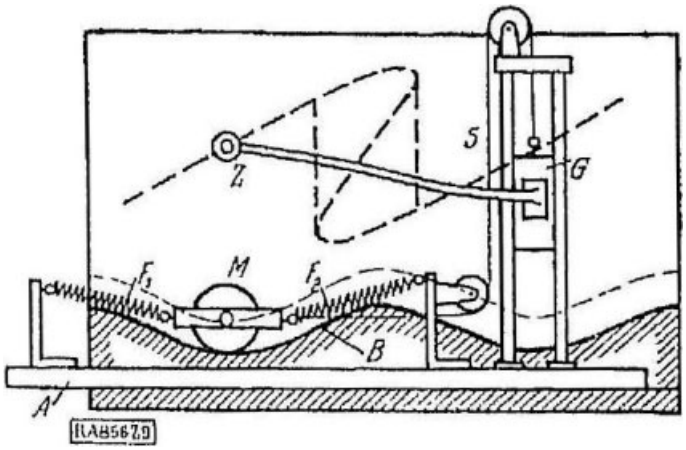

Fig. 9

After this observation of the behavior of a single point mass, we go back to our actual model, which contains a large number of point masses. It could be assumed that the waves in the force field occur at irregular intervals, being found at different positions and having different heights. We initially want to choose only regions of the force field which all have the same wavelength and height and, for the sake of simplicity, assume that the waveform and the elastic attachments of the particles are the same. Even for such a specific type of element, there should still be a very large number present. The resting points C of the point mass (see Fig. 4) would now, however, be randomly distributed over the various phases of the wave. Therefore, we will assume that they are equally distributed over the entirety of the wavelength. If we consider

the congruent sections of the waveform of the force field in the case that they coincide with one another, then we obtain a statistical distribution of stable positions according to Fig. 6, which are, of course, not completely unambiguous; which particular positions are present will generally depend on the history.

3. Performing the first-order approximation (Hysteresis). The following notations may now be introduced: Let the abscissa in the static system B (wavelike field of force) be x and let the force field in the diagram according to Fig. 6 (force dependent on the resting position C) be $P_R = f(x)$. Let the initial resting point of the point mass or – in other words – the resting point of the particles in the moving system A (straight edge with the elastic bonds) be x_0. Let the displacement of the straight edge A with respect to the field of force B be ξ. Then, for every mass particle, $x = x_0 + \xi$. Let the probability density vary between 0 and 1. In the unique case, it is $= 1$; where two stable positions are present, let $x = \mu$ for the "upper curve" and $x = 1 - \mu$ for the "lower curve." More than two stable positions are possible, but they should not be taken into consideration here. The probability of one curve can only change at the jump position, namely at the end of the other curve ("end" always taken in the sense of the immediate direction of motion) and then becomes 1 (due to uniqueness). Therefore, within the two-valued domain, μ is a function of x and is arbitrary, as long as we are dealing with the initial state. If the field of force is periodic, as we have assumed, then we need only consider one period (length $= 2l$).

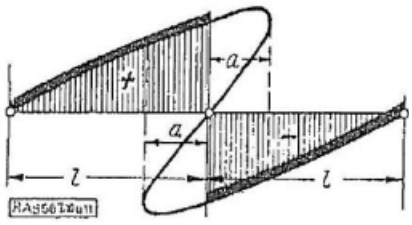

Fig. 10

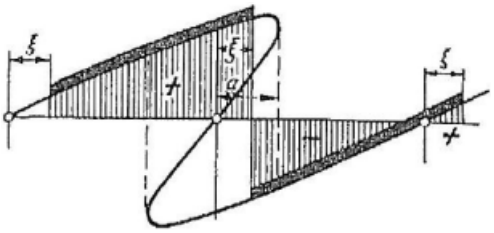

Fig. 11

If one assumes for the initial unloaded state that every point mass is in the most stable position (which, for example, can be thought of as being achieved through annealing, where slowly decreasing intensive thermal motion offers every particle the opportunity to find its most stable position), then one obtains the distribution in Fig. 10. The resulting force is shown here by the shaded region and is $= 0$. A displacement ξ smaller than the critical distance a results in the distribution shown in Fig. 11. The newly occupied distance of length ξ can, thereby, be reallocated to the end of the left side so that the outer boundaries of the distribution have not been changed. The positive area, however, has increased and the negative has decreased. Therefore, a positive force is produced. The increase in area can be represented by the shaded region in Fig. 12. In this figure, it is easy to recognize that the force is nearly proportional to ξ.

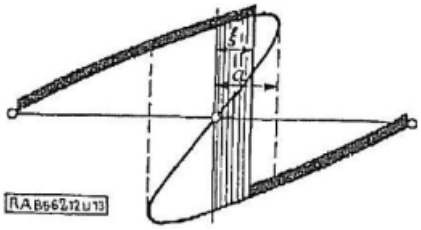

Fig. 12

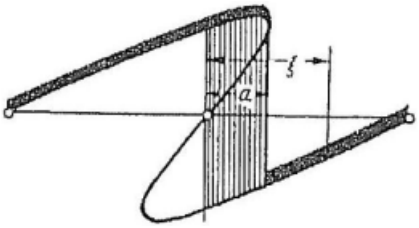

Fig. 13

For positive and negative displacements ξ whose magnitude is smaller than a, the process is reversible. For displacements $> a$, the distribution jumps over to the other branch according to Fig. 7 and the area no longer changes, so that the force remains the same as for $= a$, see Fig. 13. If the direction of the displacement were reversed at a point ξ_1, then the lower distribution changes along the other path, which corresponds to Fig. 8. Along this path, the motion is reversible until the point $\xi_1 - \xi = 2a$, at which the system jumps back to the upper curve. The resulting curve of the total force P dependent on ξ is shown in Fig. 14: It increases until $\xi = a$; then is constant until the reverse point ξ_1, where it then decreases. At $\xi = \xi_1 - a$, the force equals zero; from this point on, the force is negative; and from $\xi = \xi_1 - 2a$, constant. If one chooses now a second reverse point ξ_2, then one again obtains the positive limiting value of the force after retracing the path $2a$, such that $\xi = \xi_2 + 2a$. With a further increase in displacement, the first reverse point is transversed and the curve proceeds as if the cycle between ξ_1 and ξ_2 had never taken place. So, one sees that our model accurately satisfies Madelung's Laws.

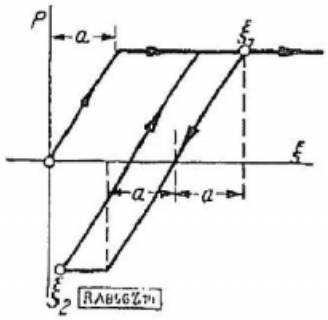

Fig. 14

Let us return to the general model with a force field consisting of waves of various amplitudes and wavelengths! This transition simply results in an assembly of various amplitudes and wavelengths in a single model, where we again ask ourselves how large the total force is which stems from all mechanisms together. As all of the mechanisms have a different "elasticity limit" a, the harder ones (larger values of a) will still remain in a reversible state, when the softer ones (smaller values of a) have already exceeded their elasticity limits. Using a suitable mixture of various hard elements, every arbitrary hysteresis loop may be achieved. Without impairing the model, one can assume the elasticity and wavelength of every element to be the same, producing different values of a using only the amplitude. If $F(\xi)$ is a force law according to Fig. 14, especially $F(\xi, a)$, for those elements with an elasticity limit of a and the distribution function $\varphi(a)$, then the total force becomes

$$= \int_0^{a_1} \varphi(a)\, F(\xi, a)\, da = \Phi(\xi).$$

As everything here is additive, Madelung's laws, which are valid for all values F, are also valid for Φ. If all elements are in the position from Fig. 10 (virgin state) at the beginning, then the elasticity limit of every element is reached when ξ is equal to the value of a of this element. After a reverse point, however, the return path is $2a$ until the elasticity limit is once again exceeded; from this, it easily follows that the virgin curve, also in the general case, is a diminished copy by a factor of $1:2$ of the loading curve beginning at the reverse point.

The question arises of how one can reproduce the virgin state after an arbitrary pretreatment of the crystal. If one allows the displacement ξ to oscillate back and forth about the middle point ξ_0 with the amplitude ξ_1, then all elements for which $a > \xi_1$ experience a reversible process and all those for which $a < \xi_1$ are brought from one resting position (Fig. 13) to the opposite. Those for which $a = \xi_1$ oscillate exactly within their limits. If one provides an oscillation with slowly decreasing amplitude, then every element whose a is smaller than the initial amplitude ξ_1 finds itself in its middle position after the oscillations have ceased. If the amplitude decreases more rashly, then it comes, at the very least, into the vicinity of its middle position. The elements for which $a > \xi_1$, in contrast, are only reversibly unloaded by the magnitude ξ_1. Upon being loaded again up to $\xi = \xi_0 \pm \xi_1$, the curve exhibits virgin behavior with a new ξ_0. Beyond this point, however, the curve shows the same behavior as a system with the same pretreatment but without oscillations. Thus, the experimentally obtained hysteresis laws prove, by our consideration, to be based on the deepest nature of the processes.

4. Second approximation (time effects). We want to denote the results that we have achieved with our conceptual model up to this point, which include the effects of hysteresis, however, does not account for time effects, as a first order approximation. The second approximation must also include time effects. It can be shown that these effects are also able to be explained by means of theoretical considerations.

We assume that every solid body exhibits heat oscillations. The amplitude of these fluctuations is not constant, but rather it is stochastically subject to fluctuations, increases at some points, decreases at others. In a few rare cases, the amplitude can become exceptionally large; these large amplitudes are to what we now want to primarily focus our attention. They can bring a particle which is still a finite distance from a position of jumping over into an instable position (D'' in Fig. 4), from which it automatically swings over to the other stable position (D''') and remains here because its oscillatory energy is damped by its surroundings. The energy U necessary for the transition is equal to the work which must be provided in order to reach the stable position acting against the difference in the forces P_B and P_A over the path $D'D''$, which corresponds to the shaded region in Fig. 4. In the representation in Fig. 6, this area corresponds to the area to the right of $F'F''$ (here also shaded)[8]. For the probability that the energy due to thermal motion becomes larger than U, the kinetic theory of matter

[8] Translator's note: This area was not shaded in original.

provides the simple formula

$$W = \mathrm{e}^{-\frac{U}{U_m}},$$

where U_m is a specific average value of the oscillatory energy of the particle. The probability becomes extremely small when U is reasonably larger than U_m; full certainty exists, probability $= 1$ for $U = 0$, meaning that $U = 0$ will be crossed-over in every case. Now, we need only to know the time in which it takes for one distribution of oscillatory energy to transfer over to another independent distribution; this time, which may be on the same order of magnitude as the period of the oscillations of the particles, should be named τ. Whether or not it is dependent on the corresponding energy may remain uninvestigated; at any rate, it shall be viewed here as being constant. With the help of the two quantities just mentioned, an ansatz can be formulated for the change of a given distribution μ with respect to time.

If N particles of a subsystem are in a specific position x inside of the force field and, from them, μN lie in the upper position and $(1-\mu)\,N$ in the lower position, then, for every time interval τ, $\mu N \mathrm{e}^{-\frac{U_1}{U_m}}$ particles, on average, transfer from the upper position to the lower position. In contrast, $(1-\mu)\,N\mathrm{e}^{-\frac{U_2}{U_m}}$ transfer from the lower position to the upper position because the number of transfers is proportional to the number of particles present in the respective initial position. Thereby, U_1 is the necessary energy needed for reaching the instable position from the upper position, while U_2 is that needed from the lower position[9]. We obtain the number of transfers per unit time by multiplying the upper value by $1/\tau$. Thus, the increase in the number of particles in the upper position with respect to time $\frac{d}{dt}(\mu N) = N\frac{d\mu}{dt}$ is equal to the number of transfers from the lower position to the upper position minus the number of transfers from the upper position to the lower position; when we divide the equation by N, we obtain

$$\frac{d\mu}{dt} = \frac{1}{\tau}\left((1-\mu)\,\mathrm{e}^{-\frac{U_2}{U_m}} - \mu \mathrm{e}^{-\frac{U_1}{U_m}}\right). \tag{1}$$

For a time-dependent change in the displacement of the straight edges with respect to one another ξ, our N particles maintain their positions against straight edge A, so that x_0 for each is fixed. Therefore, because of $x = x_0 + \xi$ (see Fig. 3),

$$\frac{dx}{dt} = \frac{d\xi}{dt}.$$

The above derivative $\frac{d\mu}{dt}$ for bound particle (fixed x_0) is, therefore, to be differentiated from the partial derivative $\frac{\partial\mu}{\partial t}$ for a fixed x. Taking into account the preceding relationship, we have

$$\frac{d\mu}{dt} = \frac{\partial\mu}{\partial t} + \frac{\partial\mu}{\partial x}\cdot\frac{\partial\xi}{\partial t}. \tag{2}$$

U_1 and U_2 are functions of x; let the deformation speed $\frac{d\xi}{dt} = c\,(t)$ be a given function of time, common for the entire system. From this ensues a partial differential equation for $\mu\,(x,t)$, which can, in principle, be solved for every given initial distribution $\mu\,(x,0)$ and every given time dependence of the deformation $\xi\,(t)$. The sum (integration) over one subsystem yields the corresponding partial force as a function of time; the sum over all subsystems yields the total force. The dependence of the processes on the temperature of the material is contained within this calculation because the temperature is proportional to the average internal energy U_m. Therefore, if one lets the internal energy assume various values in Eq. (1) or perhaps vary as a function of time, then every heat treatment before or during loading can be emulated. Incidentally, the effect that an increase of temperature has, is that the number of transfers due to the decrease in the ratio U/U_m is greatly increased and the transfers, which were previously highly improbable, are now considerably more probable.

From the preceding text, it can be recognized that our Eq. (1) allows for the behavior of a given element to be generally calculated for all problems in which the deformation is a function of time. If the complete history is known [the progression of ξ and U_m for all preceding times][10], then it is not necessary to know the initial distribution of μ. The problem for which the progression of force is given as a function of time cannot, on the other hand, be calculated directly, yet is possible in the most important case, that of elastic aftereffects, to obtain solutions using step-by-step approximations. How other problems of this type may be approximately handled based on the results of the calculations with the given deformation will be indicated in the last section. Of course, the mathematical implementation of the calculations is, as are most, bounded by the necessary time expenditures. Some cases which are able to be easily conducted, yet reveal substantially important features, are presented in the following.

[9] It is assumed that after the jump, the transfer energy of the neighboring elements is dissipated so rapidly that no neighboring element jumps immediately after. Such processes perhaps play a role in the internal of a crystal in allowing the development of plastic deformation.

[10] If the material was at a very high temperature, then it is sufficient to consider the history beginning at this point because everything earlier is erased by the intense thermal motion in this case.

5. Calculation of relaxation and aftereffects. Relaxation can be understood as the abatement of stress when a body is deformed and its form subsequently held constant. Thus, we must set $\xi = \text{const}$; the initial distribution of μ can still be assumed to be arbitrary:

$$\mu(x,0) = \phi(x) \quad \text{between} \quad x = \pm a.$$

Because $\frac{d\xi}{dt} = 0$ in Eq. (2), there exists for every value of x an ordinary differential equation with respect to t, which can be immediately integrated. It follows that

$$\mu = \frac{\mathrm{e}^{-\frac{U_2}{U_m}}}{\mathrm{e}^{-\frac{U_1}{U_m}} + \mathrm{e}^{-\frac{U_2}{U_m}}} + \psi(x)\,\mathrm{e}^{-\frac{1}{\tau}\left(\mathrm{e}^{-\frac{U_1}{U_m}} + \mathrm{e}^{-\frac{U_2}{U_m}}\right)}, \tag{3}$$

where $\psi(x)$ is, for the time being, arbitrary (an "integration constant" which, however, can have a different value for every value of x). For $t = +\infty$, the factor $\psi(x)$ is equal to zero. Therefore, the final distribution is

$$\mu = \frac{\mathrm{e}^{-\frac{U_2}{U_m}}}{\mathrm{e}^{-\frac{U_1}{U_m}} + \mathrm{e}^{-\frac{U_2}{U_m}}}. \tag{4}$$

Under certain circumstances, however, the time until this distribution is reached, which corresponds to complete relaxation, can be outrageously long. Only with very soft materials or at very high temperatures does the relaxation take place over times that can be practically considered. The determination of the arbitrary function $\psi(x)$ follows from the demand that for $t = 0$, where $\psi(x) = 1$, the following equation must be valid:

$$\mu_\infty + \psi(x) = \phi(x). \tag{5}$$

For bodies that are at least somewhat solid, simultaneous jumps up and down practically do not come into consideration because they require too much energy and, therefore, occur extremely rarely. In all such cases, the following can be written:

$$\mu = \phi(x)\,\mathrm{e}^{-\frac{1}{\tau}\mathrm{e}^{-\frac{U_1}{U_m}}} \quad \text{or} \quad 1 - \mu = \phi(x)\,\mathrm{e}^{-\frac{1}{\tau}\mathrm{e}^{-\frac{U_2}{U_m}}}. \tag{3b}$$

In order to progress further, one must find an expression for U_1 and U_2. If one assumes that the potential in Fig. 4 is a sine function, then one obtains a transcendental equation for the positions of the intersection points E' and E''. Therefore, $U_1(x)$ and $U_2(x)$ must be numerically or graphically ascertained. Their trends are provided in Fig. 15. One obtains a very good approximation when the upper and lower parts of the sinusoid are replaced with parabolas. Then, the curves in Fig. 6 and Fig. 15 (top) are also parabolas. The upper vertical part is $a\sqrt{a-x}$ and the area $= {}^2\!/_3\alpha\,(a-x)^{3/2}$. Under the assumption that $U_1 = U_m$, is $a - x = b$; with this, $\frac{U_1}{U_m} = \left(\frac{a-x}{b}\right)^{3/2}$. This can, accordingly, be replaced with $\frac{U_2}{U_m} = \left(\frac{a+x}{b}\right)^{3/2}$.

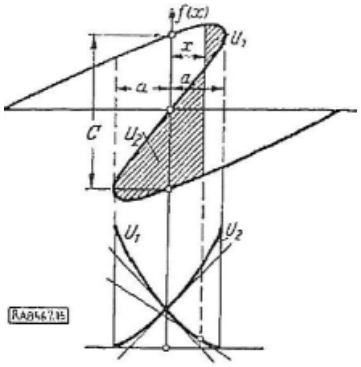

Fig. 15

With this ansatz, a very definite provision for calculation is set, which is, especially for the simplified ansatz (3a), easily accomplished. Only the integration, which is necessary for calculating the force, creates difficulties. Therefore, it is advantageous to go one step further with the simplification and approximate the law for U_1 using a linear formula (e.g., the one shown at the bottom of Fig. 15). We want to write $\frac{U_1}{U_m} = A - Bx$, where the constants can be chosen so that approximation of the straight lines is best in the domain where the most jumps occur (the largest $\left|\frac{d\mu}{dt}\right|$).

If $f_1(x)$ is the top branch and $f_2(x)$ is the bottom branch in the force curve in Fig. 15, then the total force in our subsystem becomes

$$P = \int_{-a}^{+a} [\mu f_1(x) + (1-\mu) f_2(x)]\, dx = \int_{-a}^{+a} \mu [f_1(x) - f_2(x)]\, dx + \int_{-a}^{+a} f_2(x)\, dx. \tag{6}$$

The apparent preferential treatment of $f_2(x)$ is explained in that by choosing the value μ, the two branches of the force curve are formally unequally evaluated. If, as is here always assumed, the two branches of the curve are congruent, then incidentally, $\int_{-a}^{+a} f_2(x)\, dx = -\int_{-a}^{+a} f_1(x)\, dx$, therefore, symmetry is still present[11].

One can also calculate the extra force that P has in comparison to P_∞, which corresponds to the distribution $\mu = \mu_\infty$, which also may have been present before loading. Incidentally, is $P_\infty = 0$ for congruent curves. For non-congruent curves, one would likewise claim that $P_\infty = 0$, due to physical reasons, so that $P - P_\infty$ is always equivalent to P; from this, one obtains a second expression for P:

$$P = \int_{-a}^{+a} (\mu - \mu_\infty) [f_1(x) - f_2(x)]\, dx. \tag{7}$$

Outside of the boundaries $x = \pm a$, the integral does not have to be considered because time dependent changes of the distribution are not possible here. Now, considering Fig. 15, shows that the height of the jump $f_1(x) - f_2(x)$ for all x between $-a$ and $+a$ is only slightly variable; therefore, the error is not large if it is set to be constant. Thus, we approximate the expression as

$$f_1(x) - f_2(x) = C$$

and obtain the final expression for the force in Eq. (7):

$$P = C \int_{-a}^{+a} (\mu - \mu_\infty)\, dx. \tag{8}$$

Eq. (6) now provides

$$P = C \left[\int_{-a}^{+a} \mu dx - a \right], \tag{9}$$

because

$$\int_{-a}^{+a} f_2(x)\, dx = -\frac{C}{2} 2a = -Ca,$$

where in the most probable case of $x < 0$, is $\mu = 1$ everywhere. Therefore, Eq. (9) can also be written as

$$P = C \int_{0}^{+a} \mu dx, \tag{9a}$$

which is a relation that can also easily be seen in Fig. 12. Incidentally, Eq. (8) leads likewise to Eq. (9) due to the fact that $\int_{-a}^{+a} \mu_\infty dx = a$ [compare Eq. (14) in the following]. The integrals in Eq. (8) and Eq. (9a) and the parenthetical expression in Eq. (9) may be shortened together by denoting x^* such that $P = Cx^*$. Here, x^* is the bottom line of the rectangle with a height of 1, for which the area corresponding to the integral can be calculated (compare to Fig. 16).

[11] A completely symmetric presentation is achieved by the introduction of another distribution m: $\mu = 1/2\,(1+m)$; $1-\mu = 1/2\,(1-m)$, as m goes from -1 to $+1$.

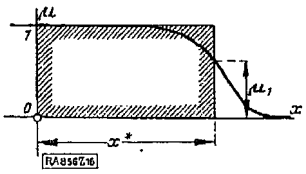

Fig. 16

Initially, we consider hard materials where the reverse jumps may be neglected. Therefore, Eq. (3a) is applicable with $U_1/U_m = A - Bx$ and $\phi(x) = 1$:

$$\mu = \mathrm{e}^{-\frac{t}{\tau}\mathrm{e}^{-A+Bx}} = \mathrm{e}^{-\frac{t}{\tau \mathrm{e}^{A}}\mathrm{e}^{Bx}}. \tag{10}$$

$\tau \mathrm{e}^{A} = \tau_1$ is now a new time constant, which is exceedingly large, for the most part, due to the large values of A in the cases considered here. The assumption that the reverse jumps may be neglected allows us to state that t is small in comparison to τ_1. For negative values of x, as well as some range of positive values, μ is practically $= 1$. Near the area, however, where $t\mathrm{e}^{Bx}$ is of the same order of magnitude as $t\mathrm{e}^{A}$, μ falls rather quickly to 0. The curves marked as $k = 500$ and $k = 50$ in Fig. 17 can be considered as the trends of μ for two times, t_1 and t_2. The curves are congruent by application of our approximation. Now,

$$\int_0^a \mu dx = \int_0^a \mathrm{e}^{-\frac{t}{\tau_1}\mathrm{e}^{Bx}} dx$$

must be calculated. Using partial integration,

$$\int_0^a \mu dx = \mu dx\,|_0^a - \int_1^0 x d\mu = \int_0^1 x d\mu,$$

due to the fact that μx vanishes for $x = 0$ as well as $x = a$ (the latter only to a practical, but still sufficient, extent!). The following results by inverting the function $\mu(x)$:

$$x(\mu) = 1/B\left\{\ln(-\ln\mu) - \ln t/\tau_1\right\}, \tag{11}$$

where it can be easily seen that the distributions belonging to two different points in time result in congruent curves, of which the curve corresponding to the later point in time can be obtained by shifting the curve correspondingly to the first point in time by $1/B \ln t_2/t_1$ to the left along the x-axis. It follows straightforwardly that in this time, the force decreases by

$$P_1 - P_2 = C/B \ln t_2/t_1. \tag{12}$$

This decrease slows but never ends and, at arbitrarily large times (according to the approximation formula), reaches arbitrarily large values. With this, practically everything that one would want to know about our model is complete. Let it be added that by the interplay of an arbitrary number of subsystems, the form of Eq. (12) once again results, since all partial contributions are proportional to $\ln t_2/t_1$. (This is not completely true if one follows the exact ansatz $\frac{U_1}{U_m} = \left(\frac{a-x}{b}\right)^{3/2}$).

The integral $\int_0^1 x d\mu$, incidentally, can be exactly calculated analytically. Using partial integration, $\int_0^1 \ln(-\ln\mu) d\mu$ can be brought into the form of the logarithmic integral function and results in a value of -0.5772 according to Jahnke-Emde p. 19*... Therewith, is

$$P = C\int_0^a \mu dx = C/B\left[\ln\tau_1 - \ln t - 0.5772\right] = C/B\left[A + \ln\tau - \ln t - 0.5772\right]. \tag{12a}$$

For soft materials (e.g., glowing hot iron), the reverse jumps must be taken into account. Here, if one sets $U_1 = A - Bx$ and U_2 (a mirror image of U_1 according to Fig. 15) $= A + Bx$, with values of A and B which approximately correspond

* No footnote in the original (remark Editor)

to the tangents at the intersection points of $U_1(x)$ and $U_2(x)$ in Fig. 15, as well as $\tau e^A = \tau_1$, then Eq. (3) provides the expression

$$\mu = \frac{e^{-Bx}}{e^{Bx} + e^{-Bx}} + \psi(x)\, e^{-\frac{t}{\tau_1}\left(e^{Bx}+e^{-Bx}\right)}. \tag{13}$$

For $t = \infty$, the resulting expression is

$$\mu_\infty = \frac{e^{-Bx}}{e^{Bx} + e^{-Bx}} = \frac{1}{2}(\tanh Bx). \tag{14}$$

μ_∞ is given by the curve marked as $k = 0$ in Fig. 17, which is now no longer congruent to the earlier μ curves.

According to Eq. (8), we must find $\int_{-a}^{+a} (\mu - \mu_\infty)\, dx = x^*$. For $t = 0$, we now leave $\mu = 1$, which only means that in the past there were much larger loads than those currently present. Therefore, as stated above, $\psi(x) = 1 - \mu_\infty$. It would be informative to follow the entire transition from the earlier approximation to the current more rigorous solution, however, the integration cannot be conducted in general. Therefore, let us investigate only the very last stage. The factor $e^{Bx} + e^{-Bx} = 2\cosh Bx$, which is next to t/τ_1, is the smallest at $x = 0$, which is $= 2$. It increases rashly with increasing distance from $x = 0$, which means that $e^{-\frac{2t}{\tau_1}\cosh Bx}$ is the largest at $x = 0$ for time t on the order of magnitude of τ_1, but decreases very strongly to both sides. Thus, only a part of the distribution around μ_∞ remains, whose extent in the x-direction is on the order of $1/B$ and whose height at $x = 0$ is given by $1/2e^{-\frac{2t}{\tau_1}}$, due to the fact that $\mu_\infty(0) = 1/2$. With this, the integral $x^* = \int (\mu - \mu_\infty)\, dx$ is on the order of magnitude of $\frac{1}{2B} e^{-\frac{2t}{\tau_1}}$ and the corresponding force, $= Cx^*$, on the order of magnitude of $\frac{C}{2B} e^{-\frac{2t}{\tau_1}}$. This expression formally agrees with the Maxwell equation for the relaxation[12]. Thereby, the time $\tau_1/2$ plays a role in the Maxwell relaxation time.

For a system that is composed of a number of such elements, the anticipated force is

$$P_t - P = \sum A_i e^{-\frac{2t}{\tau_i}}. \tag{15}$$

It is very difficult to observe the relaxation. However, the observation of elastic aftereffects, which are related to the relaxation, lead to the laws of the form of Eq. (12) or Eq. (15). The latter was derived on the basis of experiments by Weichert[13] and was discussed extensively. The former was observed by Bennewitz on bent glass fibers[14].

The elastic aftereffects, which deal with the changes in form during constant loading or after such a loading, belong to a set of problems which are no longer directly able to be solved using our formulas. However, the following considerations lead to an approximate solution. We imagine a model constructed of many elements, the overwhelming majority of which are only elastically loaded for the processes in question. A small number, however, experience inelastic loadings due to their low yield stress. In this case, the change of the form will be decided, for the most part, by the elastic elements. For inelastic elements, the change of the form can be considered as given. For a constant loading or a load of zero, this deformation is constant for a first-order approximation; the relaxation of the "soft" elements can be considered to occur at a constant ξ. Therefore, the formulas developed here are also applicable for the elastic aftereffects if the body behaves essentially elastic and only small deviations from elastic behavior are investigated. To be exact, the elastic elements experience a change in the total force under which they are loaded, due to the relaxation of the softer elements and, therefore, a change in the displacement ξ. This quantity ξ is exactly what is observed in the aftereffects. One can naturally think of calculating a second order approximation by using the time dependent changes in ξ from the first order approximation; however, actually conducting these calculations would prove to be quite difficult. Our calculations show us in which cases Eq. (12) and in which Eq. (15) are applicable. If the time constant τ_1 (relaxation time, compare to p. 96) is large in comparison to the observation time, then we can expect a behavior according to Eq. (12). If, on the other hand, τ_1 or τ_i is on the order of magnitude of the observation time, then Eq. (15) is applicable.

6. Calculation for constant deformation rate. For technical applications, the study of yielding by a given deformation rate is more important than the elastic aftereffects. Here, we investigate especially the simplest case of this type, steady state yielding by a constant deformation rate. Let the deformation rate be c; due to steady state, we set $\frac{\partial \mu}{\partial t} = 0$. With this, we obtain Eq. (2):

$$\frac{\partial \mu}{\partial t} = c\frac{\partial \mu}{\partial x}.$$

[12] Scientific Papers Vol. 2, p. 26 (Cambridge 1890).

[13] Ann. d. Phys. U. Chem. Bd. 50 (1893), S. 546.

[14] Physikal. Zeitschr. Bd. 21 (1920), S. 108. It may, hereby, be mentioned that the improbably small time constant τ from Bennewitz (order of magnitude 10^{-200} sec) can be eliminated if one adds an elastic deformation component proportional to loading to the Bennewitz formula.

With this value, the time no longer appears in Eq. (1); an ordinary differential equation for μ dependent on x is all that remains. This differential equation is of the first order and linear with respect to μ, therefore, solvable by integration. However, the solution in the general case is not carried out conveniently. It is simple, however, if the reverse jumps are able to be neglected; in this case, the variables are able to be separated. If one proceeds directly to the simplest formula

$$U/U_m = A - Bx,$$

then Eq. (1) assumes the form

$$\frac{1}{\mu}\frac{d\mu}{dx} = -\frac{\mathrm{e}^{-A}}{c\tau}\mathrm{e}^{Bx}, \quad \text{or after integration,} \quad \ln\mu = -\frac{\mathrm{e}^{Bx}}{Bc\tau_1} + \text{const.}$$

Thereby, we use the fact that $\tau\mathrm{e}^{A} = \tau_1$. The integration constant should be chosen so that μ goes from 0 to 1, or $\ln\mu$ goes from 0 to $-\infty$. For $x = -a$, due to the large value of B, e^{Bx} is practically $= 0$. Therefore, the constant is set to 0, and therewith,

$$\mu = \mathrm{e}^{-\frac{1}{Bc\tau_1}\mathrm{e}^{Bx}}. \tag{16}$$

The distribution is of the same type as for the relaxation, see Eq. (10). Furthermore, τ_1 is a very large time so that e^{Bx} must also be very large, in order to prevent a marked deviation of $\ln\mu$ from zero.

Now, the integral over the distribution must be found. It should be somewhat similar to Eq. (9a). The calculation is, once again, the same as for relaxation; we must only substitute $1/Bc$ in the place of t. Therefore,

$$P = \frac{C}{B}\left(\ln B\tau_1 + \ln c - 0.5772\right) = \frac{C}{B}\left(A + \ln B\tau + \ln c - 0.5772\right). \tag{17}$$

The interplay between many elements changes nothing about the type of dependence of the force on the deformation rate; for two speeds, c_1 and c_2, there is a difference in the total force of

$$P_2 - P_1 = \text{const} \cdot \log c_2/c_1. \tag{18}$$

The dependence of the force on the velocity c, therefore, has the form which was anticipated by observations. Eq. (17) and Eq. (18) have the peculiarity that for $c = \infty$, the force is logarithmically infinite and for $c = 0$, has a negative logarithmic singularity, which is physically absurd. It must, however, be pointed out that in order to perform this derivation (compare to the previous section), it was assumed that μ is practically $= 0$ for $x = a$ and practically $= 1$ for $x = 0$. This is true, however, only between certain limits of c, which, for the most part, lie fairly far away from one another. This behavior for very large velocities is shown by the fact that within our first approximation, the largest force is $P_{\max} = Ca = \frac{CA}{B}$, or a distribution of $\mu = 1$ to $x = a$, respectively. The equation for the case of $\mu(a) > 0$ is not easily determined, but can be integrated analytically. The case of small values of c will be handled in the following. Here, the reverse jumps must be taken into account. Because of this, the preceding calculation is only suitable for values of $Bc\tau_1$ that are approximately larger than 10 (compare to Fig. 18).

Let it be mentioned that for the case of moderate values of c (no reverse jumps), even with the more exact formula of

$$\frac{U}{U_m} = \left(\frac{a-x}{b}\right)^{3/2},$$

an analytical approximation can be obtained. In this case, integrating Eq. (1) results in

$$\ln\mu(x) = -\frac{1}{c\tau}\int_{-\infty}^{x} \mathrm{e}^{-\left(\frac{a-x'}{b}\right)^{3/2}} dx'. \tag{19}$$

(The lower limit of the integral, which should actually be $= -a$, can be set to $= -\infty$ practically without changing anything.) If we use the shortcut $z = \frac{a-x'}{b}$, then

$$b\int_{z_1=\frac{a-x}{b}}^{\infty} \mathrm{e}^{-z^{3/2}} dz$$

must be calculated. This is

$$\int\limits_{z_1=\frac{a-x}{b}}^{\infty} \mathrm{e}^{-z^{3/2}} dz = 2/3 \frac{\mathrm{e}^{z_1^{3/2}}}{\sqrt{z_1}} \left(1 - \frac{1}{2z_1^{3/2}} + \frac{1}{z_1^3} - \frac{7}{2z_1^{9/2}} + \dots\right).$$

Usually, all but the first term of the series are able to be neglected. With this, the following approximation is obtained

$$\mu(x) = \exp\left[-\left(2b\mathrm{e}^{-\left(\frac{a-x}{b}\right)^{3/2}}\right) \Big/ \left(3c\tau\sqrt{\frac{a-x}{b}}\right)\right]. \tag{20}$$

In the discussion of this formula, we are interested primarily in the domain of x in which the principal part of the transition from $\mu = 1$ to $\mu = 0$ takes place. The approximate middle of this domain is found if Eq. (20), for instance, is solved for x with $\mu = 1/2$, which is, however, only possible using successive substitution of an approximated value of x and subsequently improving the equation. In addition, one can search for the breadth of the transition domain. This is approximately $= 1/\left|\frac{d\mu}{dx}\right|$ for an average μ. It is simple to prove that $\frac{d\mu}{dx} = \frac{3}{2}\mu \ln \mu \cdot \frac{c\tau}{\sqrt{(a-x)b}}$. Therefore, with $\mu = 1/2$, $1/\left|\frac{d\mu}{dx}\right| = \frac{4}{3\ln 2} \cdot \frac{\sqrt{(a-x_1)b}}{c\tau}$. Both the numerator and the denominator work towards the fact that for increasing velocities, in other words, approaching the point $x_1 = a$, the transition becomes even more steep.

Instead of integrating Eq. (20), which could only be numerically carried out for the isolated case, one can obtain an approximate value for x^*, by determining the value of x in Eq. (20) that corresponds to the appropriate average value μ_1 of μ. Thereby, one can set $\mu_1 = 1/2$; or better, one takes a value which by using the same technique on Eq. (10) and Eq. (16), leads to the result of Eq. (12a) and Eq. (17), namely, $\ln(-\ln \mu_1) = -0.5772$, $\mu_1 = 0.5704$. Now, the task is to solve either Eq. (19) or Eq. (20) for x, respectively, with $\mu = \mu_1$. The trend of Cx^*, dependent on c, results in the desired expression for force.

If one wishes to study the dependence of the force on temperature, then one observes the fact that U_m is proportional to the absolute temperature T; U_1/U_m is, therefore, inversely proportional to the temperature if it is assumed that the force field, $U_1(x)$, is not changed by temperature. In reality, the thermal expansion would cause certain changes; however, they are not too considerable. If they were not to be considered, then the temperature effects can be taken into account by using the following formulas: $U_1/U_m = A - Bx$, $A = A'/T$, and $B = B'/T$, where A' and B' are now two constants which are independent of temperature. For the force corresponding to a given deformation rate, Eq. (17) is

$$P = \frac{C}{B'}\left\{A' + T\left(\ln\frac{B'\tau}{T} + \ln c - 0.5772\right)\right\}. \tag{21}$$

(Due to the relationship $P_{\max} = CA/B = CA'/B'$, the term inside the parentheses is always negative, so that P decreases with increasing temperature). The "creep resistance"[15] could be calculated by assuming that in a time t_1, 100 years for instance, the deformation by creep can be, at the most, equal to the elastic deformation at the yield point, or

$$\xi_1 = c_1 t_1 = a; \quad c_1 = a/t_1.$$

Thereby, due to the logarithmic input dependence, there is not much of a difference if the assumptions change somewhat. By experimentation, one would perhaps choose the largest time available for the observation for t_1 and the smallest detectable deformation for the corresponding ξ_1. With $\ln\frac{B'\tau}{T_1} + \ln c_1 - 0.5772 = -K$, we obtain the resulting creep resistance

$$P_1 = C/B'\left\{A' - T(K + \ln T/T_1)\right\}. \tag{22}$$

The term $\ln T/T_1$ is usually insignificant so that in a first-order approximation, there is a linear decrease with temperature. What is more important in this task is to use the more exact expression for U_1, namely that $U_1 = \mathrm{const}\,(a-x)^{3/2}$. Here, a rough estimation may be enough. The value of U_1, at which most transitions occur, can be seen approximately as a multiple of U_m (dependent on the deformation rate) and is then itself proportional to the absolute temperature. Therewith, is $(a-x)^{3/2} = \mathrm{const} \cdot T$, or

$$x = x^* = a - \mathrm{const} \cdot T^{2/3}$$

[15] The term was introduced by F. Koerber and means the corresponding loading for which still no lasting deformation occurs, refer to F. Koerber, Zeitschr. f. techn. Physik Bd. 8 (1927), S. 421.

(x^* being that of the earlier meaning). From this, a force is obtained:

$$P = Cx^* = Ca - KT^{2/3}. \tag{23}$$

Now, the case of especially small deformation rates and especially large heat transfers must be handled, respectively, where the reverse jumps must be taken into account. We limit ourselves here to the ansatz $\frac{U_1}{U_m} = A - Bx$, $\frac{U_2}{U_m} = A + Bx$. Taking into account that which was discussed in Sect. 4, the resulting differential equation is obtained:

$$\frac{d\mu}{dx} = \frac{1}{c\tau_1}\left[(1-\mu)\,\mathrm{e}^{-Bx} - \mu \mathrm{e}^{Bx}\right], \tag{24}$$

where $\tau_1 = \tau \mathrm{e}^A$ is once again the (usually very large) time constant $= 2 \times$ Maxwell Relaxation Time.

For deformation rates so small that $c\tau_1$ is small compared to $1/B$, a series expansion can be conducted for $Bc\tau_1 = k$. We set $Bx = y$ and obtain the following from Eq. (24):

$$k\frac{d\mu}{dy} = \mathrm{e}^{-y} - \mu\left(\mathrm{e}^{y} + \mathrm{e}^{-y}\right). \tag{24a}$$

This equation can be solved by setting $\mu = \mu_0 + k\mu_1 + k^2\mu_2 + \ldots$ and, in each case, setting the terms with the same exponents equal to each other. Therefore,

$$\mu_n = -\frac{1}{\mathrm{e}^y + \mathrm{e}^{-y}} \cdot \frac{d\mu_{n-1}}{dy} = -\frac{1}{2\cosh y} \cdot \frac{d\mu_{n-1}}{dy}. \tag{25}$$

Calculating the zero degree terms with respect to k results in

$$\mu_0 = \frac{\mathrm{e}^{-y}}{\mathrm{e}^y + \mathrm{e}^{-y}} = \frac{1}{2}\left(1 - \tanh y\right). \tag{25a}$$

This distribution is identical to that after the relaxation process is completed; (here denoted as μ_∞; here, it is the limiting distribution as the deformation rate approaches zero after a sufficient amount of time (infinitely long in the mathematical sense). The recursion formula provides

$$\mu_1 = \frac{1}{4\cosh^3 y} \quad (25\text{b}), \qquad \mu_2 = \frac{3}{8}\frac{\sinh y}{\cosh^5 y} \quad (25\text{c}), \qquad \mu_3 = \frac{3}{16}\frac{\left(5\sinh^2 y - \cosh^2 y\right)}{\cosh^7 y}. \tag{25d}$$

Now, to calculate the force (the boundaries of $\pm Ba$ can be replaced by $\pm\infty$ practically without error, because $\mu_0 = \mu_\infty$ is able to be omitted and the remaining terms on both sides rapidly approach zero if $|y|$ is reasonably large). The terms μ_2, μ_4, etc. are odd, therefore, the integral from $-\infty$ to $+\infty$ is $= 0$; by lengthy integration, the even terms yield[16]

$$\int_{-\infty}^{+\infty} \mu_1 dy = \frac{\pi}{8}, \quad \int_{-\infty}^{+\infty} \mu_3 dy = -\frac{3\pi}{256}.$$

With this, inserting the value for k results in

$$P = \frac{\pi}{8} C c\tau_1 \left(1 - \frac{3\left(Bc\tau_1\right)^2}{32} + \ldots\right). \tag{26}$$

Therefore, we obtain the very noteworthy result that in the case of a very small value for the dimensionless quantity $Bc\tau_1 = Bc\tau \mathrm{e}^A$, the force P is proportional to the deformation rate; thus, a resistance of the same type as the drag in a fluid exists. The correction term located in the parentheses indicates the first deviation from linear behavior (compare also below to Fig. 18). The trend of μ according to Eq. (25a) and Eq. (25b, c), on one side, and Eq. (16), on the other side, show the two left curves and the two right curves in Fig. 17, respectively. The solid curves 1 and 2 in Fig. 18 show the trend of the total force according to Eq. (17) and Eq. (26). Unfortunately, the two curves leave out a seemingly long section in the middle. This section is bridged by calculating the numerical solution to Eq. (24a) for the values $k = 3$, $k = 5$, and

[16] I thank Mr. Walter Tollmien for conducting this seemingly cumbersome calculation.

$k = 10$[17]. The points obtained in this fashion are plotted in Fig. 18 (made recognizable by circles). Using these points and the connecting curve between the curves 1 and 2, the dashed curve 3 is sufficiently defined as an extension. The trend of μ for $k = 5$ is taken for the average value in Fig. 17. Fig. 19 shows the trend of $y^* = Bx^* = P \cdot \frac{B}{C}$ dependent on k for four different scales of k. The k-values are written on each curve. The trend of the force dependent on the velocity $c = \frac{k}{B\tau_1}$ for large and small values of $B\tau_1$ can be easily seen in Fig. 19[18].

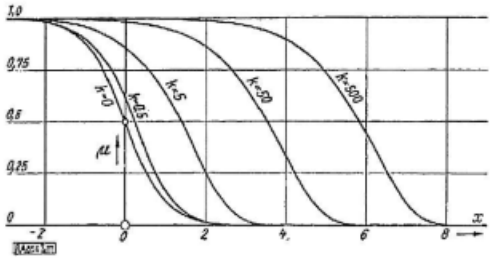

Fig. 17

In order to allow the influence of temperature to come forward, we once again set $A = A'/T$, $B = B'/T$, and $\tau_1 = \tau \mathrm{e}^{-A'/T}$; with this, the force corresponding the a deformation rate c can be found for all temperatures. If we unite the entire domain presented in Fig. 19, we obtain the complete transition from solid bodies to liquids of low viscosity including all states of softening in between, even by using our strongly simplified calculation. The limit of application of Eq. (26) moves towards larger velocities due to the fact that B, and especially τ_1, decrease significantly as the temperature strongly increases. From this behavior and for small values of c, we obtain the "viscosity"

$$\lim_{c\to\infty} \frac{P}{c} = \frac{\mu}{8} C\tau \mathrm{e}^{A'/T}. \tag{27}$$

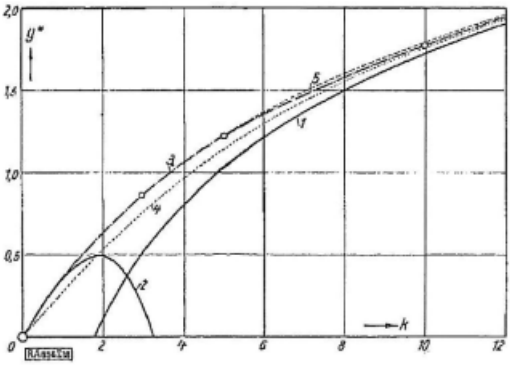

Fig. 18

For lubricating oils and other viscous liquids, a fifty percent decrease in viscosity is observed for every increase of temperature of 10 to 20 degrees. The presence of temperature in the exponential function in Eq. (27) makes it easy for this fact to be understood. Experiments by P. W. Bridgeman[19] showed, with respect to the dependence of viscosity of liquids on pressures up to about 12000 atmospheres, that the viscosity of most liquids increases dramatically (up to a factor of

[17] This calculation was conducted by Mr. Tollmien with the help of Mr. Liebehenz. Eq. (24a) is solved using the formula $\mu = \mathrm{e}^{\frac{-2\sinh y}{k}} \int_{-\infty}^{y} \frac{\mathrm{e}^{-y}}{k} \mathrm{e}^{\frac{2\sinh y}{k}} dy$. The integral for this formula was initially tabulated for the three values $k = 3$, $k = 5$, and $k = 10$ and the corresponding curves were graphically integrated using the technique of average abscissa and then applied to the formula. In the middle part, the accuracy was good, but not in the asymptotic transitions to the values $\mu = 1$ and $\mu = 0$. For this, the plot of Eq. (24a) was drawn, which like every first order linear differential equation, has the convenient property that all lines through points with a common abscissa run through a fixed point. The resulting curves were then smoothed.

[18] In some cases, the approximation formula may be desired that runs from $k = 0$ until $k = \infty$. The simplest way is to solve for y^* with $2 \cdot \mathrm{e}^{0.5772} = 3.562{:}k = 3.562 \sinh y^*$. This is shown in Fig. 18 by the dashed line 4; it is only roughly correct for small k. One can, however, improve it using an additional term so that the initial tangent agrees with Eq. (26). This challenge is satisfied using the formula $k = 3.562 \sinh y^* - 1.01 \frac{y^*}{1+y^{*2}}$. The trend of this curve is shown as the dashed line 5 in Fig. 18. For y^* as a function of k, the following formula is applicable:

$$y^* = \operatorname{arcsinh} \frac{k}{3.562} + 0.45 \frac{k}{4+k^2}.$$

The corresponding curve is so close to curve 5 that it must be left out in order to keep from obscuring the plot.

[19] Proc. Of the Amer. Acad. of Arts and Sciences Vol. 61 (1926), p. 57, compare also Verhandl. d. II. internat. Kongresses für techn. Mechanik, Zürich 1926, S. 63 ff.

one thousand and more). He determined that the increase in viscosity can be approximated using a geometric series if the pressure is increased according to an arithmetic series. If one assumes that the wave height of our force field, and with it the transition work A', is proportional to pressure (with this high pressure, the free volume is decreased), then the behavior of Eq. (27) is approximately exponential (only approximately because the value C is also dependent on pressure).

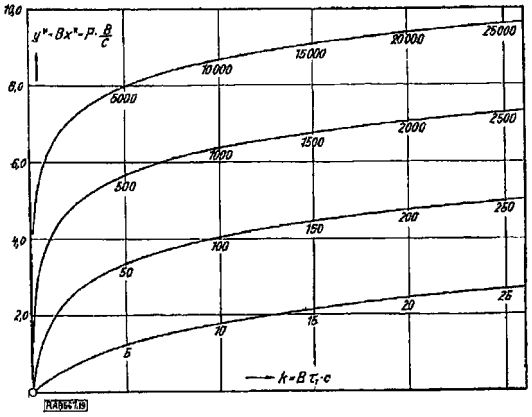

Fig. 19

For he who investigates the strength of solid bodies, the processes at the beginning of deformation away from the stress-free state, initially or as a continuation after a resting period, as well as those from one deformation rate to another may be of interest. Such processes can be basically determined according to the preceding theory. If one sets $\frac{d\xi}{dt} = c$ and x_0 as the initial position, then $x = x_0 + ct$. If now x_0 and t are seen as independent variables, then $\frac{d\mu}{dt} = \frac{\partial \mu}{\partial t}$ should be inserted into Eq. (1) because x_0 is constant for each particle. With this, at least for the case in which the reverse jumps can be neglected, an integral form of the solution is immediately possible. For the ansatz $U_1/U_m = A - Bx$, Eq. (16) becomes

$$\mu\left(x_0, \tau\right) = \psi\left(x_0\right) \mathrm{e}^{-\frac{1}{Bc\tau_1} \mathrm{e}^{B\left(x_0 + ct\right)}}.$$

In order for $\mu = \phi\left(x_0\right)$ at $t = 0$ to be true, it is obvious that

$$\psi\left(x_0\right) = \phi\left(x_0\right) \mathrm{e}^{\frac{1}{Bc\tau_1} \mathrm{e}^{Bx_0}}.$$

The force $P\left(t\right)$ can, therefore, be calculated by numerical integration for every individual value of t. The loading history has an impact on the distribution $\phi\left(x_0\right)$. A closed-form general solution is, as one can see, not able to be assigned here, however, due to the dependence on the loading history, it is also not principally possible. Therefore, we will present a crude technique in the following which admittedly misapplies the influence of the processes that are associated with the loading history. It may also be said that we will digress from the model with this technique and only use a final formula (Eq. (18)) in the future, which the model affords, as if it were valid in every case, although it was derived for a steady yielding state in our model. We now want to, purely phenomenologically, arrange the deformation corresponding to a stressed state as the sum of an elastic and an inelastic component. For the sake of simplicity, let it be assumed that the inelastic component never decreases. To show that we are no longer dealing with our model, let us once again denote the stress with σ (instead of P, as in the model) and the deformation with ε (instead of ξ, as in the model). Let the elastic component be $\varepsilon_1 = \sigma/E$, with $E =$ the modulus of elasticity. It should be valid for the inelastic component ε' that the rate of its increase $\frac{d\varepsilon}{dt}$ is related to the stress according to Eq. (18). While introducing a new characteristic time τ' (a very large time with respect to the earlier τ_1, let $\sigma = \mathrm{const} \cdot \ln\left(\tau' \cdot \frac{d\varepsilon'}{dt}\right)$ with β being the inverse of the constant; the inverse of this equation is

$$\frac{d\varepsilon'}{dt} = \frac{1}{\tau'} \mathrm{e}^{\beta\sigma}. \tag{28}$$

By setting $\varepsilon = \varepsilon_1 + \varepsilon' = \frac{\sigma}{E} + \varepsilon'$, is $\frac{d\varepsilon}{dt} = \frac{1}{E}\frac{d\sigma}{dt} + \frac{1}{\tau'}\mathrm{e}^{\beta\sigma}$. If ε is assumed to be a function of time, or more generally a function of t and σ, then this becomes a first order differential equation for σ and t. Let us offer here, as an example, the solution for the case $\frac{d\varepsilon}{dt} = c = \mathrm{const}$, beginning with $\sigma = 0$ at $t = 0$. The solution is

$$\sigma = \frac{1}{\beta}\left[\ln c\tau' - \ln\left(1 + c\tau' \mathrm{e}^{-\beta E c t}\right)\right]. \tag{29}$$

For small times, the 1 in the second logarithm may be neglected due to the very large value of τ'; therewith, the formula simplifies to $\sigma = ECt = E\varepsilon$, meaning purely elastic behavior. In contrast, the second logarithm gradually decreases for

large values of t due to the fact that $\ln(1+u) \approx u$ and the stress approaches the steady-state value of $\sigma_1 = \frac{1}{\beta} \ln c\tau'$. The time constant of the decay of the non-steady stress component is obviously $\tau'' = 1/E\beta c$ and the corresponding deformation, $c\tau'' = 1/E\beta$, which is independent of deformation rate c. This means that stress-strain curves corresponding to the transition during sudden changes of deformation rate are congruent to one another if the direction of the transition is the same. This can also be directly seen from Eq. (29) if one replaces ct with ε. This behavior is also verified in experiments for cases in which there is no disturbance from hardening, crystal regeneration, or similar processes. The revisions to the calculation that would be necessary to account for the changes associated with such processes have not yet been investigated. Incidentally, the simplicity of Eq. (28) also allows the results of various other processes to be calculated which are unassailable in the more exact method, for instance, the case in which a rod in a tensile testing machine remains at a particular length after the machine is stopped, while with progressively increasing deformation, the stress in the machine gradually decreases. Let us, however, not go further into this topic here.

7. Overview and Outlook. We have come to the close of the examination of the conceptual model. It is worthwhile to summarily ask what has been achieved with these endeavors, and contrariwise, what has not been achieved. The model has proven to be very suitable for demonstrating typical hysteresis and aftereffects, and furthermore, the interplay between the various types of aftereffects. This model is still no trustworthy representation of the atomic structure existing within a genuine solid body. Nevertheless, it is hopeful that the interaction between the various processes that have here been theoretically brought to bear will be generally confirmed in realistic solid bodies. These relationships at least give a direction in which it is worthwhile devoting research. Should this research deliver something unexpected, diverging from the model, then one knows that some effect has come into play that cannot be properly explained with this model. Among these effects, for instance, is hardening. On can, in fact, present single-sided hardening which is connected to the softening in the opposite loading direction if one assumes that some elements remain infinitely elastic. This is, however, a very artificial assumption which can hardly depict the actual processes. Two-sided hardening, meaning hardening also associated with hardening in the opposite loading direction, can in no way be presented by this model. This is obviously related to the fact that we are dealing with the processes in the lattice structure of the body, which are only to be understood spatially but are lost in the transition to the straight edge analogy. Crystal regeneration, meaning the reversal of the disorder produced by the deformation, which can be seen by the reversal of hardening, can be equally poorly presented. Recrystallization, meaning the complete reconstruction of stress-free crystals from deformed crystals and crystals under stress, insofar as this process influences hardening, can likewise not be presented. On the contrary, the gradual ebbing of the present stress as well as the steady plastic flow under moderate loading depicts a certain analogy with the thermal jumping of the particles in the model. Therefore, under favorable conditions we can, more or less, expect good agreement between the model and the actual behavior, while in a crystalline body undergoing plastic flow, there will be competition between the hardening and softening due to recrystallization.

The model assumes the existence of disorder in the initial state of those particles that are the bearers of the deformation motion. These elements should, according to our assumptions, be evenly distributed over all phases of the force field, which is fulfilled in the mean by complete disorder by the law of large numbers. Thus, it is expected that our equations are correct, above all, in such cases where the deforming movements are present primarily in the grain volumes. Furthermore, it is expected that even for such materials whose spatial construction consists of complete disorder, as with such amorphous materials as glass, tar, etc., the equations of the model are correct, including thermal behavior. For crystalline materials, on the other hand, insofar as the deformation involves the grain boundaries, a consistent result cannot be anticipated. Perhaps, a different approach would lead to the obtaining of a better model. It could, for instance, be assumed that elements be regularly placed along straight edge A with respect to the force field, however, at the same time, coupled with differing elasticities. In this way, the interaction of the particles over the lattice structure is taken into account. It is conceivable that by assuming an original defect (somewhere, a position is skipped or doubly-occupied), certain properties (shear stress during the translation of a single crystal) can be calculated, where the thermal effects must once again be observed. These calculations would, admittedly, require means other than what is here conveyed and it is not yet certain whether their complexities may be mastered.

In order to introduce hardening into the model, one can consider that the model consists of several railway tracks, laid out in a way such that every element proceeds along its track over continually steeper mountains and valleys, and on the return trip the elements travel through switches and arrive upon additional tracks where the mountains and valleys are yet steeper, etc. Crystal regeneration and recrystallization can be, thereby, introduced in that the elements may also make jumps, due to heat oscillations, perpendicular to the tracks, after which the elements return to the low mountains and shallow valleys. Meanwhile, this construction is liberally artificial and its mathematical execution, not very alluring. The seed of thought is able to be usefully exploited, however, in a form connected to the analysis presented in Sect. 6.

We want to understand hardening in such a way that the material, through permanent deformation in increasing quantities, is transformed into a structural state in which it exhibits a higher degree of hardness. We want to denote the fraction

of the "phase" with the higher strength with z; $z = 0$ would, thereby, correspond to a completely unhardened material and $z = 1$, to material completely transformed into the hardened phase. In the simplest case, we can now write the following in place of Eq. (28):

$$\frac{d\varepsilon'}{dt} = \frac{1}{\tau'} \mathrm{e}^{\beta\sigma - vz}, \tag{30}$$

where it should once again be assumed that the we are dealing only with processes for which ε' never decreases.

The ansatz in Eq. (30) obviously has the effect that the stress, which delivers a specific $\frac{d\varepsilon'}{dt}$, becomes larger as z increases. Now, a statement about z is afforded. The simplest assumption is that one sets z proportional to ε'. This already qualitatively provides certain typical effects correctly. Better, however, is to establish that the multiplication rate of the phase z is proportional to the corresponding amount of the material which remains in the first phase, meaning proportional to $(1 - z)$. Incidentally, the increase dz should be proportional to the corresponding $d\varepsilon'$. If one wants to account for crystal regeneration and recrystallization, then one can add a spontaneous reverse transformation from the harder phase into the softer, which one logically sets proportional to the present amount of the phase with the higher strength z. In this way, we obtain

$$\begin{aligned} & dz = \lambda\,(1 - z)\,d\varepsilon' - \mu z dt, \\ \text{or} \quad & \frac{dz}{dt} = \lambda\,(1 - z)\,\frac{d\varepsilon'}{dt} - \mu z. \end{aligned} \tag{31}$$

The total deformationε is once again composed of the sum of a part dependent only on the stress $f\,(\sigma)$ (purely elastic or also including hysteresis) and one of the inelastic deformation ε'. The deformation $\varepsilon = f\,(\sigma) + \varepsilon'$ may once again be given as a function of t and σ. Therewith, a system of equations is again obtained whose integration can provide us important clues about the simplest case of hardening with and without regeneration ($\mu > 0$ or $\mu = 0$. In a dissertation[20], I have had this system applied to the time-dependent deformation of zinc rods and seemingly satisfactory consistencies of these observations with the calculations could be ascertained. The values τ'[21], β, λ, μ, and ν are the characteristic parameters of the zinc (τ' influences the height of the yield point, $1/\beta$ is the increase in stress upon doubling the deformation rate, and $\frac{\nu\lambda}{\beta}$ is the increase of stress due to hardening in the vicinity of $z = 0$, see below; λ is the quickness with which z approaches the value of 1, and μ, the regeneration). $1/\mu$ is a time constant and, as τ', is expected to be highly temperature dependent, namely, in the same way of the dependence of the time constant in the model: $\tau_1 = \tau \mathrm{e}^{A'/T}$. At the time being, the temperature dependence of the remaining values is not known. How the systems (30) and (31) work may be briefly shown here with the simplest example $\frac{d\varepsilon'}{dt} = c$, which admittedly only has practical meaning in the case that the elastic component of the deformation rate can be neglected with respect to the plastic component. Initially, Eq. (30) gives $\sigma = \frac{1}{\beta}\,(\ln c\tau' + \nu z)$; Eq. (31) provides the trend of z by integrating the exponential function of time, namely

$$z = \frac{\lambda c}{\lambda c + \mu} \left(1 - \mathrm{e}^{-(\lambda c + \mu)t}\right). \tag{32}$$

With this, the asymptotic final state $z = \frac{\lambda c}{\lambda c + \mu}$ provides the following dependence of the stress on the deformation rate:

$$\sigma_1 = \frac{1}{\beta} \left(\ln c\tau' + \frac{\nu}{1 + \mu/\lambda c}\right). \tag{33}$$

The small value of c discussed earlier, c_1, once again provides a formula for the creep resistance from this equation. One sees that for very small values of μ (very slow regeneration) the hardening value ν has an influence on the strength. In contrast, this influence vanishes for large values of μ (higher temperature). At the beginning ($t = 0$, $z = 0$ and $\frac{dz}{dt} = \lambda c$; in other words, for small times in a first-order approximation, $z = \lambda c t = \lambda\varepsilon'$, with which $\sigma = \frac{1}{\beta}\,(\ln c\tau' + \nu\lambda\varepsilon')$.

Another noteworthy type of behavior is shown by simple mild steel with its "upper yield strength" and "latent hardening" in the pauses between deformations. Here, one must assume that alongside ordinary hardening (measured through z, there is a softening which is brought about by deformation and over time, again vanishes on its own accord. One can understand this by imagining fissures appearing in the crystal due to the deformation which once again anneal in periods of rest. Let us denote the measure of softness as y. For undeformed materials, the following is once again valid: $y = 0$ and $z = 0$. The peculiar effects of the decrease of stress at the beginning of inelastic deformation come about due to the fact that the

[20] O. Brezina, Untersuchungen über die Zeitgesetze der unelastischen Deformation bei Zink und Flußeisen. Göttinger Diss. 1922. Auszug in Phys. Zeitschr. 24 (1923), S. 338.

[21] Brezina used the notation a for $1/\tau'$, the remaining correspond to those used here.

softening proceeds more quickly than the hardening. There is, however, an upper limit to softening: when everything is soft, or $y = 1$. Then, the hardening begins to become visible. The decrease in stress gives rise to an instability in the deformation process. Short sections of rods complete the entire deformation, while others remain undeformed. Deformation bands are formed. Not until this is fulfilled by the entire specimen does the hardening proceed. Until then, the stress remains constant. After long periods of rest, one finds an increase in the yield stress, which is again lost after minimal further deformation. All of these effects can be described with the following assumptions:

$$\frac{ds'}{dt} = \frac{1}{\tau'} \mathrm{e}^{\beta\sigma + xy - \nu z}, \quad (34) \qquad \frac{d\gamma}{dt} = \lambda_1 (1-y) \frac{d\varepsilon'}{dt} - \mu_1 y, \quad (35) \qquad \frac{dz}{dt} = \lambda_2 (1-z) \frac{d\varepsilon'}{dt} - \mu_2 z. \quad (36)$$

For mild steel at a reasonable temperature, one could set $\mu_2 = 0$; μ_1 corresponds to a regeneration time of a few days or weeks which, however, can be decreased to a few hours after mild heating. The softening coefficient $x\lambda_1$ is significantly larger than the hardening coefficient $\nu\lambda_2$. In the case of $\frac{db'}{dt} = c$, Eq. (32) is once again valid for z as well as a corresponding equation for y so that the time-dependent stress curve can be given for every constant deformation rate. Naturally, it should not be said that with these formulas, the entirety of the secrets of mild steel are exhausted, especially since testing through experimentation must still be conducted. It is also questionable whether one can get by with the use of linear equations (even with these, a mutual influence of z and y could be supposed). It is, for instance, conceivable that the reason for the striking elevation of the yield stress of iron between 100 and 200 degrees is that the regeneration rate μ_1 increases very strongly with the temperature so that the softening y then remains almost at the zero point. The formula for the creep resistance, analogous to Eq. (33) shows, at any rate, such an increase with temperature through the increase of μ_1. For higher temperatures, an increase in μ_2 and a decrease in τ' are also noticeable, where the recovery of hardening and recrystallization come into effect.

To conclude, it may now be suggested that our conceptual model is also suitable for the treatment of kinetic friction between solid bodies. This model is even better adapted for application to the case of two straight edges sliding against one another than for the case of plastic deformation. In reality, many experiments nowadays[22] show a behavior exactly consistent with our Eq. (18) in terms of the dependence of kinetic friction on sliding velocity (at least for small velocities and moderate loads). Naturally, there are deviations if the loads are so large that plastic deformation occurs or filings are produced. In the case of pure metallic or glass surfaces, but also between leather and iron in many cases, the law that frictional force increases with the logarithm of velocity is confirmed very well in a large range of velocities. The approximate proportionality of the frictional force with the normal force with which the bodies are pressed together may be associated with the fact that, on one hand, the effective contact surface of both bodies increases with the normal force, and on the other hand, through the increase in surface pressure, the molecules of both bodies are brought into closer proximity, and thus, a force field with larger wave amplitudes is present. A quantitative approach to this conception is still left to be done. In the context of our model, an investigation of the behavior of the frictional force dependent on temperature would be very informative under conditions, naturally, where no oxidation or similar processes occur. If this was investigated using our model, a behavior is expected such as that in Eq. (21) or in a more exact calculation associated with Eq. (20). The friction must, at any rate, significantly decrease at high temperatures. The peculiar observations seen in wheel-rail contacts and in brake pads, which show that frictional forces are only a fraction at high velocities as those which occur at lower velocities[23], are perhaps associated with the extreme heating of the actual contact surfaces between the rail or brake pad and the wheel[24].

In this manner, an entire realm unfolds in which the relationships attained here can be of use.

8. Summary. Using the conceptualization of a straight edge onto which mass elements are elastically mounted and which is axially displaced alongside another straight edge having a force field of attractive and repulsive forces, makes it possible to emulate the processes taking place in a body subjected to deformation to the point that hysteresis, elastic aftereffects, and the dependence of the yield stress on the deformation rate are in good agreement with the observed physical laws. Also in the case of temperature dependence, the complete transition of solid bodies to liquids in a state of low viscosity through the process of softening can be observed. The correct type of dependence of temperature and pressure is obtained for the viscosity of a liquid. This theory does not contain all that is associated with hardening. For this purpose, phenomenological ansätze are given. It was shown that the majority of the obtained formulas can be applied to dry friction.

[22] Charlotte Jakob, Diss. Königsberg 1911. Ann. d. Phys.(4) 38 (1912), S. 126 (brass, glass). – R. Skutsch, Dingl. Polyt. Journal 329 (1914), p. 273, 306, 341, 355 (leather on iron). – G. Sachs, Diese Zeitschrift. Rd. 4 (1924), S. 1 (leather on cast iron).

[23] Compare e.g. Hütte Bd. I, 25. Aufl., S. 282.

[24] It is possible that one reason for the decrease in frictional force is that the particles are no longer able to find the most stable positions at large speeds, and therefore, they are more easily dragged along the surface than they would be if they found themselves in the most stable positions.

